

**IND06 MIQC**

**Best-practice guide**

**Characterisation  
of  
optical components of  
weak-coherent-pulse  
Quantum Key Distribution systems**

v1.0

September 2014



This document presents current best-practice for characterising the optical components used in weak-coherent-pulse QKD systems which use phase encoding at telecom wavelengths. Particular attention is given to the single-photon sources and detectors used in such systems. The described methods are limited to those which can be implemented using commercially available, traceably calibrated instrumentation, or instrumentation that does not require the expertise of a national metrology laboratory to set up.

Christopher Chunnillall, National Physical Laboratory (NPL), United Kingdom  
Ivo Pietro Degiovanni, Istituto Nazionale di Ricerca Metrologica (INRIM), Italy  
Stefan Kück, Physikalisch-Technische Bundesanstalt (PTB), Germany  
Alastair Sinclair, National Physical Laboratory (NPL), United Kingdom

The authors acknowledge funding from project MIQC (contract IND06) of the European Metrology Research Programme (EMRP). EMRP is jointly funded by the EMRP participating countries within EURAMET and the European Union.

The authors also acknowledge extensive discussions with the ETSI Industry Standardisation Group on Quantum Key Distribution (ETSI ISG-QKD).

# Contents

Definitions.....	6
Abbreviations.....	7
1. Single-photon sources and detectors .....	9
1.1 Single-photon sources.....	9
1.2 QKD single-photon sources.....	9
1.3 Single-photon detectors .....	9
1.4 QKD detectors .....	10
1.5 QKD transmitter properties for which measurement guidelines are provided.....	12
1.6 QKD receiver properties for which measurement guidelines are provided .....	19
1.7 Measurements during operation .....	27
1.7.1 Single-photon transmitter .....	27
1.7.1.a Measurements can be carried out at single-photon level.....	27
1.7.1.b Measurements cannot be carried out at single-photon level .....	27
1.7.2 Single-photon receiver.....	27
2. Single-photon source characterisation.....	28
2.1 Clock frequency.....	28
2.1.a Equipment required .....	28
2.2 Optical pulse repetition rate.....	28
2.2.a Equipment required .....	28
2.2.b Measurement before attenuation to single-photon level.....	28
2.2.c Measurement at the single-photon level.....	29
2.3 Mean photon number of pulses emitted by QKD transmitter .....	30
2.3.1 Measurement with a calibrated power meter.....	30
2.3.1.a Required equipment.....	31
2.3.1.b. Spectrum.....	31
2.3.1.c. Power.....	31
2.3.1.d. Pulse repetition rate .....	32
2.3.1.e. Calculation.....	32
2.3.2 Measurement with a gated photon counter .....	32
2.3.2.a. Equipment required .....	32
2.3.2.b. Pulse-pair considerations.....	33
2.3.2.c. Spectrum.....	34
2.3.2.d. Pulse repetition rate .....	34
2.3.2.e. Measurement of emitted pulses .....	34
2.3.2.f. Calculation .....	35
2.4 Mean power of pulses emitted by QKD transmitter.....	36
2.4.1 Direct measurement with a calibrated power meter .....	36
2.4.1.a Required equipment.....	36
2.4.1.b Power.....	36
2.4.1.c Calculation.....	37
2.4.2 Measurement of $\mu$ .....	37
2.5 Source power stability .....	37
2.6 Source timing jitter .....	38
2.6.1 Measurement at single-photon level.....	38
2.6.1.a Required equipment.....	38
2.6.1.b Measurement .....	39
2.6.1.c Calculation.....	39
2.6.2 Measurement prior to attenuation to single-photon level.....	39
2.6.2.a Required equipment.....	39

2.6.2.b.1	Measurement with oscilloscope.....	40
2.6.2.c.1	Calculation .....	40
2.6.2.b.2	Measurement with counter/timer .....	41
2.6.2.c.2	Calculation .....	41
2.7	Source wavelength.....	41
2.7.a	Equipment required .....	41
2.7.b	Measurement .....	42
2.7.c	Calculation.....	43
2.8	Spectral linewidth .....	43
2.9	Spectral indistinguishability .....	44
2.9.a	Required equipment.....	44
2.9.b	Measurement .....	45
2.9.b.1	Fixed phase pattern.....	45
2.9.b.2	Random phase pattern .....	46
2.9.c	Calculation.....	46
2.10	Temporal profile .....	46
2.10.a	Required equipment.....	46
2.10.b	Measurement with oscilloscope.....	47
2.10.c	Measurement with counter/timer .....	47
2.10.d	Calculation.....	47
2.11	Temporal indistinguishability .....	48
2.12	Single-photon emission efficiency (Grangier parameters and pulse-to-pulse stability).....	48
2.12.a	Equipment required.....	48
2.12.b	Measurement.....	48
2.13	Polarisation state.....	49
2.13.a	Equipment required.....	49
2.13.b	Measurement.....	49
2.13.c	Calculation .....	50
3.	Single-photon detector characterisation .....	51
3.1	Clock frequency.....	51
2.1.a	Equipment required .....	51
3.2	Detector gate repetition rate .....	51
3.3	Detector gate detection probability profile .....	51
3.3.a	Required equipment.....	51
3.1.b	Measurement.....	51
3.1.c	Calculation of detection probability profile?.....	52
3.4	Dark count probability (per gate).....	52
3.4.a	Required equipment .....	52
3.4.b	Measurement.....	52
3.4.c	Calculation .....	52
3.5	After-pulse probability .....	52
3.5.a	Required equipment (all fibre-coupled).....	53
3.5.b	Measurement.....	55
3.5.c	Calculation .....	56
3.6	Detection efficiency .....	57
3.6.a	Measurement.....	57
3.4.b	Calculation.....	57
3.7	Linearity factor (detection efficiency).....	58
3.7.a	Measurement.....	58
3.7.b	Calculation.....	58
3.8	Spectral responsivity .....	58
3.9	Dead time, recovery time, partial recovery time, reset time .....	59

3.9.a	Required equipment (all fibre-coupled)	59
3.9.b	Measurement	60
3.9.c	Calculation	61
3.9.d	Dead time	61
3.9.e	Recovery time	61
3.9.f	Partial recovery time	61
3.9.g	Reset time	62
3.10	Maximum count rate	62
3.12.a	Equipment required	62
3.12.b	Measurement	62
3.11	Timing jitter	62
3.13.a	Required equipment	63
3.13.b	Measurement	64
3.13.b.1	Measurement with oscilloscope	64
3.13.c.1	Calculation	64
3.13.b.2	Measurement with counter/timer	64
3.13.c.2	Calculation	65
Appendix 1		66
Appendix 2		68
Appendix 3		69
Appendix 4		70
References		71

## Definitions

Terms not listed here will be defined within the body of this document.

Alice:	quantum information sender/transmitter in a QKD system
Bob:	quantum information receiver in a QKD system
classical channel:	communication channel that is used by two communicating parties for exchange of classical information
click/no-click:	refers to detectors that are not photon-number-resolving
detection deficiency:	$1 - \text{detection efficiency}$
detection probability:	probability of registering a signal when a pulse of given mean photon number is incident on the detector
Eve or eavesdropper:	any adversary intending to intercept communication between Alice and Bob
intensity modulator:	device that can actively set the intensity of an optical pulse that is passing through the modulator
mean photon number:	the average number of photons per pulse
phase modulator:	device that can actively set the phase of a photon that is passing through the modulator
power meter:	device which measures incident optical power
QKD session:	set of all raw bits which are subject to one particular round of sifting, error correction, and privacy amplification, to generate a particular secret key
quantum channel:	communication channel for transmitting quantum signals
quantum photon source:	optical source for carrying quantum information
single-photon detector:	device that transforms a single-photon into a detectable signal with finite probability
spectrometer:	device for measuring the spectrum of optical pulses
traceable calibration:	calibration that is based on the SI
weak laser pulse:	optical pulse obtained through attenuating a laser emission

## Abbreviations

AMZI	Asymmetric Mach-Zehnder Interferometer
APD	Avalanche PhotoDiode
APP	After-pulse probability
BB84	QKD protocol published by Bennett and Brassard in 1984
BNC	Bayonet Neill-Concelman connector
CV	Continuous Variable
DC	Direct current
DCP	Dark count probability (per gate for gated detectors, per second for free-running detectors)
DE	Detection efficiency
DUT	Device under test
FWHM	Full-width at half-maximum
HBT	Hanbury Brown - Twiss
MIQC	Metrology for Industrial Quantum Communications
NIM	Nuclear Instrumentation Module
PNRD	Photon-number resolving detector
PNS	Photon Number Splitting attack
QKD	Quantum Key Distribution
QND	Quantum non-demolition
QRNG	Quantum Random Number Generator
QST	Quantum State Tomography
SM	Single Mode
SMA	Sub-Miniature version A connector
SNSPD	Superconducting nanowire single-photon detector
SPAD	Single photon avalanche photodiode
SPC	Single-Photon Counting
SPDC	Spontaneous Parametric Down-Conversion
SPS	Single-photon source
TTL	Transistor-Transistor Logic



# 1. Single-photon sources and detectors

## 1.1 Single-photon sources

A true single-photon source will emit individual photons at periodic intervals. To guarantee its operation, the core of the source will be a solitary quantum emitter such as an atomic particle, molecule, or quantum dot. Deterministic emission is triggered by a periodic electronic or optical excitation of the source. An ideal source will exhibit highly-efficient polarized emission into a well-defined spatial optical mode; there will be negligible temporal jitter of the photon emission with respect to the clock signal triggering the emission.

## 1.2 QKD single-photon sources

The most commercially advanced QKD systems operate over optical fibre, use attenuated laser pulses ('faint pulses') as an approximation to true single photons, and encode information on the phase of the photons[1]. Photons are distributed in attenuated laser pulses according to Poissonian statistics, hence some pulses will contain two or more photons. In order to reduce the power of photon-number-splitting (PNS)[2] attacks on these multi-photon pulses, the SARG [3] and decoy state [4] protocols were developed.

For pulses with a particular mean photon number  $\mu$ , the probability of there being  $n$  photons in any single pulse can reasonably be assumed to follow the Poissonian distribution, i.e.

$$p(n, \mu) = \frac{\mu^n}{n!} e^{-\mu} \quad (1.1)$$

where  $\mu$  is the mean number of photons in a pulse (mean photon number), and  $p(n, \mu)$  is the probability of there being  $n$  photons in a particular pulse when the mean photon number is  $\mu$ .

## 1.3 Single-photon detectors

Single-photon detectors, also referred to as photon counters, operate in either gated, or non-gated (i.e. continuously gated) modes, and are only able to detect an incoming optical pulse during these gates. Single-photon detectors can be characterised by their following properties:

- photon-number resolution (their ability to distinguish the number of photons in each detected pulse);
- detection efficiency (the probability that a photon incident at the optical input of the detector, within a detection gate, will be detected);
- dark count probability (the probability that a detector registers a detection event within a detection gate in the absence of incident photons);
- after-pulse probability (the probability that a detector registers a false detection event in the absence of illumination, conditional on a true photon detection event in a preceding detection gate);

- dead-time (the time interval after a detection event when the detector is unable to provide a response to an incoming photon);
- recovery time (the shortest time duration after a photon detection event for the detection efficiency to return to its steady-state value);
- jitter (the temporal variation in the output signal produced by the detector upon registering an event);
- linearity of response (the property that the detector response is unchanged as the number of incident photons per pulse varies over a specified range);
- maximum exposure level (the photon flux above which the detector may undergo a temporary or permanent change in characteristics).

A property that is important in QKD is the photon counter indistinguishability, i.e. the extent to which the detector output voltage pulses of detectors can be distinguished in the time domain.

An ideal detector would be photon number resolving for all  $n$ , where  $n$  is the number of photons in a pulse, as well as having unity detection efficiency, and zero dark count and after-pulse probabilities, with no dead-time or recovery time.

Various single-photon detection technologies exist, and a particular technology may only exhibit a subset of the characteristics listed above.

## **1.4 QKD detectors**

Single-photon avalanche photodiodes (SPADs) operating in Geiger mode are the most common and commercially successful solution for single-photon counting, and are commonly used in commercial and near-commercial QKD systems operating in the 1.3 and 1.55- $\mu\text{m}$  telecom regions. Si SPADs have been used in experimental short-haul systems. SPADs are preferred because they are relatively low-cost, and can operate with thermoelectric cooling, as opposed to cryogenic cooling.

SPADs are based on an avalanche photodiode structure reversely-biased above the breakdown voltage (known as Geiger mode operation), so that electron-hole pairs generated by photon absorption are multiplied in an avalanche gain process. To control this effect, the avalanche must be stopped, and the device reset by a passive or active quenching circuit.[5-8] As such, SPADs are not photon-number resolving, although low bias devices have been explored for their photon-number resolving ability.

Silicon based SPADs operating in Geiger mode achieve single-photon sensitivity in the VIS-NIR, with low dark counts and timing jitter reduced to tens of picoseconds.

SPADs for the 1.3 and 1.55  $\mu\text{m}$  telecommunication bands use lower-band-gap semiconductor materials such as Ge and InGaAs/InP.[9-13] These devices suffer from dark count rates that are orders of magnitude higher than for their Si counterparts, and are typically operated in gated Geiger mode, although free-running operation has recently been achieved.[14,15] In SPAD detectors charge carriers created during the avalanche process become trapped at atomic defect sites in the multiplication region. The subsequent de-trapping of these carriers at a later time can trigger spurious additional avalanches known as after-pulses. After-pulses are a type of dark count, but

unlike other dark counts mechanisms – such as thermal excitations or tunnelling effects – that occur randomly in time, after-pulses are strongly correlated to previous avalanches during which trap sites were populated.[16]

These devices also exhibit dead, reset and recovery times, which limit their maximum count rate. There are differing definitions of these terms in the literature, and we adopt those given by Migdall et al.[17] After a detection event, there will be a time-interval when the detector as a whole is unable to provide an output in response to incoming photons at the single-photon level, and which may be due to intrinsic processes within the detector or its control electronics. We shall call this the dead time,  $t_{\text{dead}}$ . After the dead time has elapsed, the detector is able to detect incident photons; however, it may take some further time before its detection efficiency recovers to its steady-state value. We shall call this the reset time,  $t_{\text{reset}}$ . The sum of these times we shall call the recovery time,  $t_{\text{recovery}}$  i.e.  $t_{\text{recovery}} = t_{\text{dead}} + t_{\text{reset}}$ . If the detector recovers to its normal value slowly, it may be useful to specify a shorter recovery time, where the detection efficiency is some fraction (e.g. 90% or 99%) of the final value. We shall call this the partial recovery time,  $t_{\text{partialrecovery}}$ . Note that in the literature,  $t_{\text{recovery}}$  has sometimes been defined as the dead-time.[18]

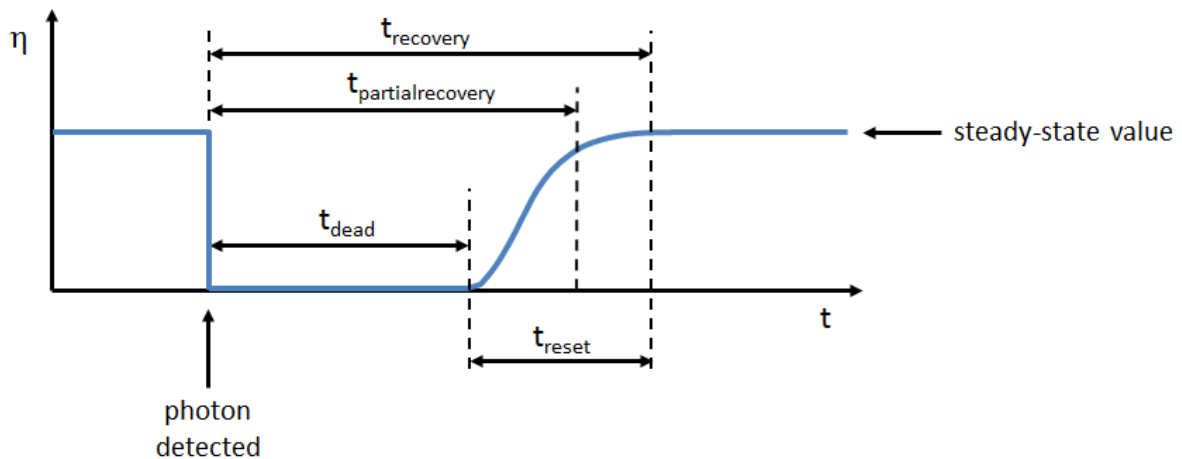


**Fig. 1.1.** Detection efficiency as a function of time. [Adapted from 17]

## 1.5 QKD transmitter properties for which measurement guidelines are provided

Parameter	Symbol	Units	Definition	Measurement approach
1. Clock Frequency	$f_{\text{clock}}$	Hz	The frequency set by the pulse generator	Measure via standard traceable time and frequency calibration techniques – e.g. measuring the pulse train with a high bandwidth oscilloscope
2. Pulse repetition rate	$f_{\text{pulse}}$	Hz	The repetition rate of the emitted pulses	Measure the light before attenuation to the single-photon level, with a high-bandwidth photodiode and oscilloscope.
3. Mean photon number	$\mu$	Photons per pulse	Average number of photons per emitted pulse	<p>(i) Measure using traceably calibrated single photon detector;</p> <p>(ii) Measure the average power with a traceably calibrated power meter, and calculate mean photon number using <math>P = nh\nu\mu</math>, where <math>P</math> is the measured power, <math>n</math> is the number of pulses per second, <math>\mu</math> is the mean photon number per pulse, and <math>\nu</math> is the mean spectral frequency of the pulses.</p> <p>Method (ii) is only suitable for a transmitter that is emitting photons with the same mean photon number, and at a sufficient rate to be measureable with a power meter. The measurement techniques rely on the detection model and the photon statistics of the source. Both assumptions should be checked.</p>
4. Source power	$P$	W	The absolute average power emitted by the laser over the time period of a QKD session	Direct measurement by using a calibrated power meter
5. Source power stability		dB/hr	The variation in source intensity over the period of 24 hours	Stability measurement using calibrated power meter or single photon detector depending on the pulse repetition rate, and whether the measurement is performed before or after the signal is attenuated to the single photon level.
6. Source timing jitter	$J_S$	s	The uncertainty in the emission time of a photon at the optical output.	<p>In considering an attenuated laser source, two options for jitter measurements are available:</p> <p>(i) The attenuated source with its output at the single-photon level can be detected by a superconducting nanowire detector, since the jitter of such detectors is low (<math>&lt; 100</math> ps) in comparison to other detectors [19]. By correlating many successive detection events</p>

				<p>with the clock signal triggering the source, a histogram of detection times will be observed. By deconvolving this signal from the detector's inherent jitter, the source jitter can be determined.</p> <p>(ii) The other approach measures the optical output pulse from the source, prior to the attenuator that reduces the flux to the single-photon level. By performing this measurement on laser pulses containing many photons, it is then possible to detect them with a fast photodiode, rather than a photon-counting detector. The photodiode has a higher bandwidth and significantly less jitter than the superconducting nanowire detector.</p> <p>If measuring the jitter of a single-photon signal using the superconducting nanowire detector, then a measurement uncertainty of <math>&lt; 50</math> ps is feasible. By measuring the jitter of the laser pulses before attenuation using a fast photodiode, a measurement uncertainty of <math>&lt; 10</math> ps is feasible.</p>
7. Source wavelength	$\lambda$	nm	Wavelength of photons that are emitted.	<p>Attenuated laser sources used in commercial quantum communication systems operate in the <math>1.3 \mu\text{m}</math> and <math>1.5 \mu\text{m}</math> regions of the near-IR spectrum. The calibration of wavemeters and the wavelength scale of optical spectrum analysers is conventionally carried out using a tunable laser such as external-cavity or distributed feedback laser which gives a single wavelength output. The laser output is locked to molecular vibration-rotation transitions of gas-phase molecules, and, in the <math>1.5 \mu\text{m}</math> region, CO and <math>^{13}\text{C}_2\text{H}_2</math> transitions are employed [HC1998, Edwards2005]. The accuracy with which a device can be calibrated depends on the spectral resolution and stability of the device under test, but for a high-quality wavemeter with resolution of <math>0.1</math> pm, or <math>1</math> pm, the achievable uncertainty can be as low as <math>0.15</math> pm, or <math>0.6</math> pm, respectively (<math>k = 2</math>).</p> <p>When the laser in the QKD source is driven to emit short optical pulses, typically <math>&lt; 100</math> ps in duration, the spectral width of the source is <math>\Delta\lambda_{\text{source}} \sim 0.1</math> nm, which corresponds to <math>\Delta\nu_{\text{source}} \sim 12</math> GHz. This will affect the accuracy with which the wavelength can be <i>measured</i>. A wavemeter suitable for use with pulsed sources can measure such a laser's centre wavelength, <math>\lambda_{\text{source}}</math>, with an uncertainty <math>\Delta\lambda_{\text{source}}</math> of <math>\sim 0.002 - 0.01</math> nm, depending on stability,</p>

				spectral profile, and S/N.
8. Spectral line width	$\delta\nu$ $\delta\lambda$	GHz nm	Bandwidth of the emitted photons.	<p>A wavemeter, or optical spectrum analyser, can also be used to measure the spectral linewidth of an attenuated laser source. In addition, two other methods are available:</p> <p>(i) By using the light emitted by the pulsed laser source, prior to the attenuator, and beating it against a tunable narrow-linewidth auxiliary laser, the spectral linewidth can be measured. The tunable narrow linewidth laser should be stabilised such that its linewidth <math>\Delta\nu_{\text{stabilised}} \leq 10</math> MHz, <i>i.e.</i> much narrower than the attenuated source (<math>\Delta\nu_{\text{source}}</math>). The spectral linewidth of the pulsed laser source will be revealed by the beatnote, observable when the auxiliary laser is tuned near the source's optical frequency. Using this beat note method, a resolution of <math>\sim 200</math> MHz, should be feasible. Note that this method is not suitable for optical pulses at the single-photon level.</p> <p>(ii) The use of a stable, tunable Fabry-Perot resonator provides another route to measuring the source linewidth. The technique requires that the cavity free spectral range (FSR) is much greater than the source's pulsed laser linewidth, <i>i.e.</i> <math>\text{FSR} \gg \Delta\nu_{\text{source}}</math>, yet have a linewidth <math>\Delta\nu_{\text{cavity}} \ll \Delta\nu_{\text{source}}</math>. When used in transmission mode, the Fabry-Perot cavity can be tuned to resonance with the pulsed laser source to record its spectral profile. When analysing the optical pulses prior to the attenuator, the signal would be measured using a PIN photodiode. The technique is also appropriate for measuring the attenuated laser pulses (containing on average one photon or less), by using a superconducting nanowire detector. For example, a pulsed laser source operating at 80 MHz repetition rate, and using the nanowire detector, good signal to noise can be achieved with the cavity resolution stated above.</p>
9. Spectral indistinguishability	$s^{\text{ind}}$	Unitless	The extent to which the encoded states can be distinguished through spectral measurement.	The spectral indistinguishability of encoded individual photons is vital to avoid any possibility of being able to detect the encoded key. For example, the spectral profile of the individual photons can be affected by the phase modulator used to implement the phase encoding scheme in the BB84 protocol (and its variants). The encoding modulator's phase is randomly changed between successive laser pulses; it is essential that this has settled at a constant value prior to the pulse propagating in the modulator, and that further switching occurs afterwards. If the phase switching (or

				<p>settling) occurs while the laser pulse is propagating through the modulator, then a changing phase shift will be experienced, and the leading edge of the pulse may see a different phase shift from the trailing edge. The spectral characteristics of the laser pulse will be distorted, and will be present on the photons transmitted in the quantum channel. It is therefore possible that with such spectral distortion, the four different encoding phases may be distinguished by spectral means. Spectral measurements are needed to demonstrate that the photons are spectrally indistinguishable, irrespective of the phase encoded onto them.</p> <p>The Fabry-Perot resonant cavity, described in the “spectral linewidth” measurement, can be used to perform this analysis. The cavity acts as a narrowband spectral filter, and by scanning the cavity length, its resonance frequency is tuned. By accumulating transmitted signals as a function of resonant frequency, the photons’ spectral profile can be determined. This should be done for each of the four encoding phases using the normal switching of the modulator. A spectral distinguishability will be evident if there is a difference between these spectral profiles. A deliberate phase change coinciding with the propagation of the laser pulse through the modulator will highlight this feature, thus demonstrating the sensitivity of the instrumentation.</p>
10. Temporal profile				
11. Temporal indistinguishability	$t^{ind}$	Unitless	The extent to which the encoded states can be distinguished through temporal measurement.	<p>The source’s temporal indistinguishability is assessed by detecting the laser’s output pulse after it has passed through the phase and intensity modulators, but before it passes through the attenuator that reduces the pulses to the single-photon level. It is not expected that temporal distinguishability will be a problem for QKD systems based on a single source to generate all signal and decoy states.</p> <p>Measurements can be performed with a fast photodiode and a wide-bandwidth oscilloscope, for various combinations of the phase modulator and intensity modulator settings. By synchronising the detection with the clock for the pulsed laser source, the fast photodiode and oscilloscope enable a sampled version of the output pulse to be obtained. By varying the combinations of the phase and intensity modulator settings, the measurement</p>

				<p>can be repeated to determine whether any temporal distinguishability is detectable. A comparison of temporal profiles can be made for each of the four encoding phases for the phase modulator, and for the attenuations set using the intensity modulator.</p> <p>Jitter may be caused by drifts in path difference, therefore all cables and fibres in the setup should be kept physically and thermally stable. An external clock should be used to synchronise the pulse generator controlling the laser source, and the oscilloscope timebase. The uncertainty in the timebase of the measuring instrument can be as low as 5 ps, and the temporal uncertainty will be dominated by the jitter of the laser pulses, which can be 10 ps or more. which can be 10 ps or more.</p>
12. Single-photon emission efficiency		Unitless	The ability of the single photon source to emit real single photons	<p>For a real (practical) single photon source (SPS) an important characterization consists in verifying the possibility of having more than one photon per pulse emitted by the source. The usual set-up used for this is the Hanbury Brown-Twiss interferometer (HBT) operating at single photon level. The HBT is typically implemented using two threshold (click/noclick) detectors placed at the output ports of a 50:50 beam-splitter, [Grangier1986, Eisaman2011, Migdall2013]</p> <p>The efficiency of a single-photon source can be described by means of the <math>\alpha</math> parameter proposed by Grangier et al. [Grangier1986]. This is essentially an ‘anticorrelation criterion’ based on the parameter:</p> $\alpha = Q(2)/[Q^{(1)}(1) Q^{(1)}(1)]$ <p>where <math>Q(2)</math> is the probability of the coincidence click between the two detectors of the HBT interferometers, while <math>Q(1)</math> is the probability of a click by one of the two detectors ((I), (II) indicate the two detectors after the beam splitter). In the single-photon community the parameter <math>\alpha</math> is often called the second order correlation function <math>g^{(2)}</math> [Grangier1986], but we prefer to call it <math>\alpha</math>, since <math>g^{(2)}</math> has a different definition [Mandel1995], despite the fact that in the few photon regime the two definitions are asymptotically equivalent.</p> <p>Despite being apparently not useful in the case of an SPS based on an attenuated laser (since the <math>\alpha</math> parameter should be equal to one, a value that is independent of the intensity of the coherent source), its estimation is important</p>

				since it provides information about the pulse-to-pulse stability of the attenuated laser output. Instabilities in energy pulses may open a security leakage in QKD systems.
13. Polarisation state (omit?)		Unitless	Light Polarisation reconstruction	<p>Photon polarisation is the quantum mechanical equivalent of the classical electromagnetic light polarisation. The quantum polarisation state vector for a single photon, for instance, is identical with the Jones vector, usually used to describe the polarisation of a classical wave. Thus, it is clear that the quantum state tomography is equivalent to the estimation of Stokes parameters for classical light, with the only difference being: instead of measuring light power, what is experimentally observed are the relative detection frequencies of single photon detection, i.e. conditional probabilities of detection of single photons. Tomographic reconstruction of the polarization state at the single-photon level is more affected by detection imperfections (e.g. dark counts, afterpulses, etc) and the fact that non photon-number-resolving single-photon detectors (operating in Geiger mode) are usually employed, compared to conventional polarimetry employing well-established light detection technology in the macroscopic regime. For this reason, proper reconstruction algorithms, such as e.g. Maximum Likelihood algorithms) should be employed to reconstruct physically meaningful polarisation state information about the single photons.</p> <p>The problem of the estimation of the uncertainties on Stokes parameters is complicated by the fact that optimisation algorithm are employed. In fact, they are not able to provide an effective estimation of uncertainty.</p> <p>The simplest solution will be developing a single-photon polarimeter similar to the design of a conventional polarimeter, where at the same time the polarization measurements in all the needed polarisation basis (i.e. horizontal/vertical, diagonal/anti-diagonal, left- and right-circular) is performed. At single-photon level this means that the signal would be detected in the best case scenario by one of the six single photon detector. The total detection efficiency of each detector in this setup is reduced by the splitting of the field, thus this measurement will be more affected by dark counts and afterpulses with respect to a measurement where, for example, only two detectors are present and the different polarization measurement projections are</p>

				performed in sequence by modifying the polarisation control systems. For this reason the single-photon polarimetry adopts the second approach. The use of gated photon counters appears to be preferable when a pulsed laser source will be used.
--	--	--	--	---

## 1.6 QKD receiver properties for which measurement guidelines are provided

Parameter	Symbol	Units	Definition	Measurement approach
1. Clock frequency	$f_{\text{clock}}$	Hz	The gate trigger frequency set by the clock	Measure via standard traceable time and frequency calibration techniques – e.g. measuring the trigger signal train with a high bandwidth oscilloscope
2. Gate frequency	$f_{\text{gate}}$	Hz	The actual frequency at which the detector is gated.	
3. Detector gate detection probability temporal profile		Unitless	The relative detection probability profile as a function of time with respect to the gate trigger.	Use CW laser radiation (at the single-photon level) to irradiate the single-photon detector, and measure the number of counts as a function of time relative to the gate trigger.
4. Dark count probability	$p_d$	gate <sup>-1</sup>  ns <sup>-1</sup>	For a gated detector this is the probability that a detector registers a detection event in a stated gate time, in the absence of optical illumination.  For a free-running detector this is the probability that a detector registers a detection event in 1 ns, in the absence of optical illumination.	The dark count probability of a detector can be measured by recording detection events per gate or per unit time in the absence of photon flux illuminating the detector's sensitive area. To perform the measurements, a counting device records the detector output signal. In order to count only detection events during gates, a time-correlated photon-counting device can be used to record the detector output signal. By correlating many dark count events with a clock signal triggering the detector gate, a time delay histogram can be observed in accordance to Yuan et al. [Yuan2007]. To calculate the dark count probability of the detector, the detected count rate will be normalised to the total number of applied gates. The uncertainty will depend on the uncertainty of the trigger clock signal and the uncertainty of the counting device, both of which can be calibrated against a traceable frequency standard, as well as the count statistics.
5. After-pulse probability	$p_{\text{after}}$	gate <sup>-1</sup>	The probability that a detector registers a false detection event in the absence of illumination, conditional on photon detection event in the preceding detection gate.	After-pulsing introduces a secondary source of dark counts, with a charge carrier production rate proportional to the trap levels. These levels have fairly long lifetimes and fairly high concentration in InGaAs/InP SPADs. As a result, the after-pulsing effect can limit the transmission rate of single photons in QKD systems.  The after-pulse probability of the SPAD can be measured in accordance with the first measurement technique described above for

				<p>the measurement of photon detection probability. Here the pulsed laser repetition rate is scaled down by an integer factor <math>R</math> compared to the detector gating rate, in order to observe detection events in the detector gates lying between the gates corresponding to consecutive laser pulses (<math>R-1</math>). A signal time-correlated photon counting technique will record a histogram of time delays between the laser trigger and the detector output. Peaks at a time delay in this histogram not corresponding to an illuminated gate are generated by photon events caused by the after-pulse effect (and dark counts). By normalising the detected count rate to the total number of applied gates, the after-pulse probability can be calculated from:</p> $P_{after} = \frac{P_{n-1} - P_{dark}}{P_1 - P_{n-1}} \cdot R$ <p><math>P_{dark}</math> is the dark count probability, <math>P_i</math> is the probability to detect a photon at each illuminated gate and <math>P_{n-i}</math> is the probability of a detection event at each non-illuminated detector gate after a previous optical excitation of the detector. The uncertainty will depend on the uncertainty of the clock frequency as well as the temporal resolution of the time-correlated photon counter, both of which can be calibrated against a traceable frequency standard, as well as the uncertainties due to <math>P_{dark}</math> and the count statistics. Uncertainties below the 1% level are achievable if the system is stable.</p>
--	--	--	--	---

6. Photon detection probability	$\eta(\nu)$ or $\eta(\lambda)$	Unitless	The probability that a photon of a specific energy (wavelength) incident at the optical input will be detected within a detection gate.	<p>Two measurement approaches can be identified, one is based on the usual substitution method, the other one exploiting an heralded single-photon source:</p> <p>(i) The photon detection probability can be measured by following the experiments carried out by Yuan et al. [20], which are also suitable for determining the after-pulsing probability and the dark count probability. Here the SPAD is illuminated by the pulsed laser source attenuated to the low photon level. Both devices are triggered by a pulse generator, whereby the laser pulse frequency is stepped down by an integer factor <math>R</math> compared to the detector gate rate. The same experimental set-up can be used to measure the after-pulsing probability <math>p_{\text{after}}</math>. A time-correlated photon counting device is used to record a histogram of time delays between the laser trigger and the detector output signal. At zero-time delay the histogram peak is dedicated to the detection events observed under laser light illumination. With the knowledge of the dark count probability <math>p_d</math> and the after-pulse probability <math>p_{\text{after}}</math> the probability photon detection efficiency <math>\eta</math> can be obtained by measuring the probability <math>p_i</math> to detect a photon at each illuminated gate as a function of the laser power. The latter is described as <math>\mu</math> photons per laser pulse on average.</p> $p_{\text{true}} = \frac{p_i - p_{\text{dark}}}{1 + p_{\text{after}}}$ $\eta = -\frac{1}{\mu} \ln(1 - p_{\text{true}})$ <p>The average number of photons per laser pulse <math>\mu</math> can be obtained by calibrating the attenuated laser source against a traceable detector standard. The latter is available for the infrared spectral region only recently; a superconducting nanowire single photo detector was calibrated against a standard InGaAs diode using synchrotron radiation with uncertainties of approx. 2 %. A practical solution is to use a calibrated detector to measure the power for a given pulse repetition rate, and then use a calibrated attenuator to reduce the pulse photon number to the single photon level. The overall uncertainty in calibrating the photon detection efficiency depends on the uncertainties due to <math>p_d</math>, <math>p_{\text{after}}</math>, <math>p_i</math>, and the count statistics. For fibre coupled devices at 1550 nm, best case uncertainties</p>
---------------------------------	--------------------------------	----------	---	---

			<p>around 2% (<math>k = 2</math>) are achievable.</p> <p>(ii) An alternative technique to the traditional one based on radiometric substitution is based on the use of parametric down-conversion to produce a heralded single-photon source. Detection of one of the down-converted photons heralds the existence of its twin, which can be directed to the device under test (DUT). This approach still suffers from multiple photon events, and various experiments [Brida2000, Polyakov2007, Cheung2011] have been carried out to demonstrate the equivalence of the two methods at the photon counting level. However, optical scales remain based on cryogenic radiometry since the lowest uncertainty so far achieved with the heralded single-photon approach (0.18%) (at single photon level, in the visible spectral region) is over an order of magnitude less accurate than that based on cryogenic radiometry (0.005%) (at the 100 <math>\mu</math>W level). This is mainly due to need to estimate the absorption in the path the heralded photon takes from the point of creation within the non-linear medium until it is incident on the detector, which may include geometrical or absorptive spectral filtering. The method also suffers from limited spectral tuneability at high accuracy. The importance of this technique lies in the fact that it establishes an absolute means of measuring detection efficiency, which is independent of cryogenic radiometry, and operates in the single/few photon regime.</p> <p>In respect of QKD receivers, the random occurrence of downconversion events means that the technique is not viable with detectors that cannot be asynchronously gated, such as SPAD detectors employing a d.c. bias just below the avalanche breakdown voltage, on top of which a high-speed periodic low amplitude bias is added. [Namekata2006, Yuan2007]</p>
--	--	--	---

7. Linearity factor (for detection efficiency)	L	Unitless	The ratio of the detection efficiency at the set power level to that at the reference power level.	The calibrated mean photon number of the attenuated laser pulses is varied (e.g. with a calibrated attenuator), and the detection efficiency is measured.
8. Spectral responsivity	$R_s$		The photon detection efficiency as a function of wavelength of the incident photons.	<p>Single-photon detectors are only sensitive over a spectral range determined by its constituting material. Within this certain spectral range their detection efficiency is a function of the wavelength of the incident photons, which is described as the detector's spectral responsivity. Losses in optical fibres are at lowest at a wavelength of 1.55 <math>\mu\text{m}</math>, which makes this wavelength favourable for uses in fibre-based QKD systems.</p> <p>To measure the spectral responsivity of the detector, its detection efficiency can be measured as described in the photon detection probability section at different wavelengths. The laser operation wavelength can be characterised by a commercial, calibrated wavemeter (0.01 nm).</p>
9. Dead time	$T_{dead}$	s	The time interval after a detection event when the detector as a whole is unable to provide an output in response to incoming photons at the single photon level.	<p>The measurement method was reported in [Kerman2006] et al., Appl. Phys. Lett. <b>88</b>, 111116 (2006).</p> <p>Optical pulse pairs of equal intensities at the single photon level are used to illuminate the detector under test. The laser pulses are synchronized to the detector gates and the relative time delay between the laser pulses only needs to be varied in steps of one gating period. At a particular time separation, detector outputs should be recorded for several pairs of incident photon pairs, where the time separation between pairs significantly exceeds the expected recovery time. The dead time is the minimum time separation at which non-zero coincidences are recorded.</p>
10. Recovery time	$T_{recovery}$	s	The smallest time duration after which the detection efficiency is independent of previous photon detection history.	<p>The measurement method was reported in [Kerman2006] et al., Appl. Phys. Lett. <b>88</b>, 111116 (2006).</p> <p>Optical pulse pairs of equal intensities at the single photon level are used to illuminate the detector under test. The laser pulses are synchronized to the detector gates and the relative time delay between the laser pulses only needs to be varied in steps of one gating period. At a particular time separation, detector outputs should be recorded for several pairs of incident photon pairs, where the time separation between pairs significantly exceeds</p>

				<p>the expected recovery time.</p> <p>The recovery time is the value of pulse separation for which the probability of measuring both pulses is the square of the probability of measuring the first pulse, i.e. the probability of measuring the second pulse is equal to the probability of measuring the first pulse.</p>
--	--	--	--	---

11. Partial recovery Time	$T_{\text{partial}}$	s	The time duration after a photon detection event for the detection efficiency to return to 90% of its steady-state value. This is only important if the detector is free running.	<p>The measurement method was reported in [Kerman2006] et al, Appl. Phys. Lett. <b>88</b>, 111116 (2006).</p> <p>Optical pulse pairs of equal intensities at the single photon level are used to illuminate the detector under test. The laser pulses are synchronized to the detector gates and the relative time delay between the laser pulses only needs to be varied in steps of one gating period. At a particular time separation, detector outputs should be recorded for several pairs of incident photon pairs, where the time separation between pairs significantly exceeds the expected recovery time.</p> <p>Usually, the rate of doubles will increase monotonically with the pulse separation, and saturate at large pulse separation. From this data, the recovery time is the pulse separation value at which the rate of the doubles reaches 90% of the saturation value. [Note that this is a simplification of the analysis for recovery time – which of the two, or both, will need to be discussed/agreed]</p>
12. Maximum count rate	$C_{\text{max}}$	Hz	The maximum rate of photon detection events under strong illumination condition in the single/few photon/gate regime.	The SPAD is illuminated by pulsed laser light at the same frequency of the detector gating rate, corresponding to an illumination pulse every detector gate. By measuring the detector count rate as a function of the photon flux, the number of detection events per gate will saturate at the detection rate limit of the SPAD. The results can be compared with the prediction of maximum count rate as a function of the detection efficiency and the dead time of the detector. The target uncertainty will be given by the measurement uncertainty of the counting device, which can be determined by a traceable frequency standard. In practice detectors are sometimes not able to achieve their maximum expected count rate (the inverse of the dead-time). This can be observed by changing in a controlled way the pulse intensities, and measuring the detection probability. A strong distortion with respect to the predicted detector behaviour will be observed just after the maximum count rate.
13. Timing jitter	$T_{\text{jitter}}$	s	The uncertainty in determining the arrival time of a photon at the optical input.	To ensure good timing resolution of a single photon detector, the time interval between the absorption of a photon and the generation of an output electrical signal should be short and stable, corresponding to a small timing jitter. A common technique to determine this parameter is to measure the full-width half-maximum (FWHM) of the detector's

				<p>instrument response function. For that purpose the FWHM of the laser pulses illuminating the detector should be narrower than the SPAD's timing jitter. By correlating many detection events with the trigger signal of the laser, a time-delay histogram can be observed by a time-correlated photon counter, from which the detector's response function can be calculated. Many detectors have non-Gaussian and asymmetric response functions, which can be taken into account in a detailed analysis. The latter will influence the target uncertainty of the measurements, as will the uncertainty of the trigger clock signal and the uncertainty of the counting device, which can be measured via a traceable frequency standard.</p>
--	--	--	--	--

## **1.7 Measurements during operation**

### **1.7.1 Single-photon transmitter**

Where measurements are to be carried out while the DUT is providing single-photons, either as a QKD transmitter, or for some other purpose, the methods described in section 2 will need to be modified as follows:

#### **1.7.1.a Measurements can be carried out at single-photon level**

A splitter (coupler) or optical switch can be used.

Where a splitter is used, the splitting ratio  $m:u$  between the measurement and user path will need to be measured, and the values obtained in the measurement channel scaled by  $u/m$  to obtain the values in the user path.

Where a switch is used, the extinction ratios for when the signal is sent to the measurement and user paths need to be measured.

#### **1.7.1.b Measurements cannot be carried out at single-photon level**

In this situation a splitter is used in the high power regime, and an attenuator is used to convert power in one arm of the splitter to the single-photon level.

The splitting ratio  $m:u$  between the measurement and user path will need to be measured, as well as the attenuation  $a$  to get to the single-photon level, and the values obtained in the measurement channel scaled by  $a*u/m$  to obtain the values in the user path.

### **1.7.2 Single-photon receiver**

Where measurements are to be carried out while the DUT is operating as a single-photon counter, either as a QKD receiver, or for some other purpose, the methods described in section 3 will need to accommodate the temporal interleaving (either gate-to-gate, or in alternate time segments) of calibration signals, and the user signals. This could be implemented using a coupler, or an optical switch. As in 1.7.1.a, the splitting ratio, or extinction coefficients of the switch, will need to be taken into account.

## 2. Single-photon source characterisation

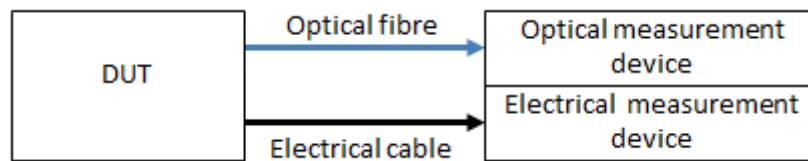


Figure 2.1 Generic experimental set-up

Optical signals are directed to the optical measurement device(s) through optical fibre, electrical signals through appropriate electrical cabling. Some measurements will only require an optical measurement device or an electrical measurement device.

### 2.1 Clock frequency

The frequency of the clock signal,  $f_{\text{clock}}$ , used to trigger the laser source in the transmitter can be measured using standard traceable time and frequency calibration techniques – i.e. by measuring the pulse train with a high bandwidth oscilloscope.

#### 2.1.a Equipment required

- (i) High-bandwidth oscilloscope

This instrument must be capable of temporally resolving the signal emitted by the clock..

### 2.2 Optical pulse repetition rate

The emitted optical pulse repetition rate,  $f_{\text{pulse}}$ , (as opposed to the laser trigger signal frequency  $f_{\text{clock}}$ ) must be confirmed by measurement.

#### 2.2.a Equipment required

- (ii) Fibre-coupled fast detector

This instrument must be capable of temporally resolving the individual pulses emitted by the DUT (before attenuation). It may be a combination of e.g. a fast photodiode and a high bandwidth oscilloscope.

#### 2.2.b Measurement before attenuation to single-photon level

$f_{\text{clock}}$  is measured with a high bandwidth oscilloscope, in order to confirm the expected optical pulse repetition rate (see Section 2.1).

For a QKD transmitter  $f_{\text{pulse}}$  is expected to be double the laser optical output rate  $f_{\text{clock}}$  because of the

embedded AMZI.

Arrangements must be made to measure the optical pulses before they are attenuated to the single-photon level. This is necessary to ensure that every pulse is measured, and so check if pulses are missed, or extra pulses produced. A fast analogue detector (the optical measurement device in figure 2.1) is connected to the DUT. The output of the fast detector is connected to a measurement device such as a high bandwidth (real-time, or sampling) oscilloscope, whose time axis has been traceably calibrated.

A pulse train is recorded, from which the pulse repetition rate  $f$  ( $\text{Hz}^{-1}$ ) is measured.

### 2.2.c Measurement at the single-photon level

Using a single-photon counter to measure the pulse repetition rate at the single-photon level is not optimal, since the combination of  $\eta_{\text{detector}} < 1$  and  $\mu_{\text{emitter}} < 1$  means that every pulse cannot be detected, and only an averaged temporal output can be measured. Therefore, random features or temporal variations in the pulse emission sequence may not be detected.

If measurements can only be carried out at the single-photon level, the following considerations apply:

- (i) A single-photon detector with a gate narrower than the shortest output pulse spacing is used as the optical measurement device. The detector should be triggered at a minimum frequency of  $f_{\text{trigger}}/n$ , where  $n$  is a positive integer ( $n \geq 1$ ). A histogram of detections versus time-delay is collected, and a tunable delay is used to synchronise one of the pulse-trains (corresponding to either the long or short arm of the AMZI) within the detector gate. The tunable delay is then further varied until the pulses from the adjacent pulse-train are detected. The tunable delay is then further varied until pulses from the first pulse-train are again detected. From the detection histogram, the time between pulses from the same pulse-train will yield the pulse repetition rate of the photon source  $f_{\text{source}}$ , and the spacing between the separate pulse-trains will give the delay between the two arms of the AMZI  $\sim 1/(2f_{\text{source}})$ .

Note that this method will only be able to confirm if there are emitted pulses at (and/or multiples/sub-multiples) of the trigger frequency

- (ii) The detector gate can be set wide enough so that  $2 \times n$  consecutive pulses (the factor of 2 is due to the AMZI) can be measured within a single detector gate, where  $n$  is a positive integer ( $n \geq 1$ ). The jitter from the detection system must be such that adjacent output pulses are resolved. [Note that a detector with such a wide gate cannot be used for the  $\mu$  measurements described lower in this section].

A histogram of detections versus time is collected, and the pulse spacing obtained. The

histogram counter and detector will be triggered at intervals corresponding to  $(n + \text{int})$  laser triggers, where  $n, \text{int}$  are positive integers ( $n \geq 1, (\text{int} \geq 0)$ )

It may be observed that there are more counts towards the start of the detector gate, since the detector may only be able to record one event within a gate.

- (iii) A continuously-gated detector can be used as the optical measurement device. Such devices are now becoming commercially available [21,22]. The detector will not need to be triggered, but otherwise, similar consideration apply as in (ii). The histogram counter will be triggered at intervals corresponding to  $(n + \text{int})$  laser triggers, where  $n, \text{int}$  are positive integers ( $n \geq 1, \text{int} \geq 0$ )

## **2.3 Mean photon number of pulses emitted by QKD transmitter**

These guidelines cover the measurement of the mean photon number(s) ( $\mu$ ) of the pulses emitted by a fibre-coupled Device Under Test (DUT) operating in the following modes:

- (a) The DUT emits pulses with the same  $\mu$ ;
- (b) The DUT emits pulses whose  $\mu$  changes according to a fixed, repetitive pattern;
- (c) The DUT emits pulses whose  $\mu$  changes randomly from pulse to pulse.

For pulses with a particular  $\mu$ , the probability of there being  $n$  photons in a pulse is assumed to follow the Poissonian distribution, i.e.

$$p(n, \mu) = \frac{\mu^n}{n!} e^{-\mu} \quad (2.1)$$

where  $\mu$  is the mean number of photons in a pulse (mean photon number), and  $p(n, \mu)$  is the probability of there being  $n$  photons in a particular pulse when the mean photon number is  $\mu$ .

It is assumed that the emission is confined to a single, continuous spectral region.

The DUT can be an assembled QKD transmitter, or a simpler device such as an attenuated pulsed laser.

In the case where the DUT is a QKD transmitter, it is assumed that the DUT incorporates an Asymmetric Mach-Zehnder Interferometer (AMZI) which splits the pulse train emitted by the photon emitter inside the DUT into a pair of pulse trains, one train being delayed relative to the other by approximately, but not necessarily exactly,  $1/(2f_{\text{source}})$ .

### **2.3.1 Measurement with a calibrated power meter.**

This method is only applicable in case (a). The emitted power from the DUT must be high enough to be directly measurable with a power meter. Otherwise, arrangements must be made to measure the optical pulses before they are attenuated to the single-photon level. In this latter case, the transmittance, from the point of measurement to the exit of the DUT, must also be measured. Where the DUT is a QKD transmitter, this method only allows the mean photon number  $\mu_{\text{both}}$ , summed over both split pulses produced by the AMZI in the DUT, to be measured.

### 2.3.1.a Required equipment

- (i) Fibre-coupled spectrometer for measuring the spectrum of the emitted pulses – this encompasses all devices capable of measuring the spectrum of the emitted pulses, and includes wavemeters, optical spectrum analysers, etc.

The spectral range of sensitivity should cover the entire spectral region over which emission occurs

The frequency or wavelength scale of the spectrometer must be calibrated traceably to the SI

The linearity of the intensity axis should be calibrated

- (ii) Fibre-coupled power meter

The optical power responsivity must be traceably calibrated to the SI at the repetition rate of the DUT pulses, and in the spectral region of interest

- (iii) Fibre-coupled fast detector

This instrument must be capable of temporally resolving the individual pulses emitted by the DUT (generally before attenuation). It may be a combination of e.g. a fast photodiode and a high bandwidth oscilloscope.

### 2.3.1.b. Spectrum

The mean spectral frequency  $\nu_m$  (Hz) of the emitted spectrum is calculated from the measured power spectrum  $P(\nu)$ .

See section 2.7

### 2.3.1.c. Power

The power meter (the optical measurement device in figure 2.1) is now connected to the DUT.

The emitted power is measured using the power meter, and corrected for any signal offset in the absence of radiation.

The corrected value is  $P$  (W)

### 2.3.1.d. Pulse repetition rate

The emitted optical pulse repetition rate,  $f_{pulse}$ , (as opposed to the laser trigger signal frequency  $f_{clock}$ ) must be confirmed by measurement.

For a QKD transmitter  $f_{pulse}$  is expected to be double the laser optical output rate  $f_{clock}$  because of the embedded AMZI.

See Section 2.2 for details of the measurement of the optical pulses before they are attenuated to the single-photon level.

### 2.3.1.e. Calculation

$\mu_{both}$  is calculated as follows:

$$\mu_{both} = \frac{P t_v}{n h \nu_m} \quad (2.2)$$

where  $\nu_m$  is the mean spectral frequency,  $h$  is Planck's constant, and  $n = 1/f_{source}$  is the number of pulses emitted by the photon emitter within the DUT in 1 second.

## 2.3.2 Measurement with a gated photon counter

This method is applicable in cases (a), (b), (c)

### 2.3.2.a. Equipment required

- (i) Fibre-coupled spectrometer for measuring the spectrum of the emitted pulses – this encompasses all devices capable of measuring the spectrum of the emitted pulses, and includes wavemeters, optical spectrum analysers, etc.

The spectral range of sensitivity should cover the entire spectral region over which the emission occurs.

The frequency or wavelength scale of the spectrometer must be calibrated traceably to the SI.

The linearity of the intensity axis should be calibrated.

- (ii) Fibre-coupled gated non-photon-number-resolving photon counter.

The detection efficiency must be traceably calibrated to the SI in the spectral region of interest

The after-pulse probability of the detector must be calibrated at the gate frequency used in the measurement

The dark count probability of the detector must be calibrated

The temporal width of the detector gate must be wider than the temporal width of the transmitter pulses, but narrower than the pulse-to-pulse spacing (see sections 2.10 and 3.1)

- (iii) Fibre-coupled fast detector.

This instrument must be capable of temporally resolving the individual pulses emitted by the transmitter (either before or after attenuation). It may be a combination of e.g. a fast photodiode and a high bandwidth oscilloscope

- (iv) Means (such as a tunable delay) for synchronising the arrival of a photon at the detector within the duration of the detector gate.

The equipment must be capable of synchronising the arrival of a photon at the detector during the detector gate, such that any jitter imparted by the synchronisation equipment maintains the arrival of a photon at the detector during the detector gate.

- (v) Means for separating the two pulse trains produced by the AMZI within a QKD transmitter (where relevant).

### **2.3.2.b. Pulse-pair considerations**

In the case where the DUT is a QKD transmitter, it is assumed that the DUT incorporates an Asymmetric Mach-Zehnder Interferometer (AMZI) which splits the pulse train emitted by the photon emitter inside the DUT into a pair of pulse trains, where one train is delayed relative to the other. This delay may not be exactly  $1/(2 \times f_{\text{source}})$ .

Each pulse train is measured separately:

This requires that one, and only one, pulse from each of the emitted pulse trains can be positioned within a detector gate.

This can be implemented if the detector gate is narrow enough to achieve this.

If this is not the case, but the detector gate is narrow enough to achieve this when one of the pulse trains is excluded from the emitted pulse stream, measurements can be carried out by excluding one, and then the other, pulse stream. In the case of systems which use polarisation to encode pulses

from the separate arms of the AMZI [23], this can be done by inserting a polarisation controller and beamsplitter/polariser at the output of the QKD transmitter. The measurements will need to be corrected for losses introduced by these extra components.

### 2.3.2.c. Spectrum

Measurement of the output spectrum is required to so as to use the correct value of  $\eta_D(\lambda)$  for the photon counter (see section 4.2.f.i).

The mean spectral frequency  $\nu_m$  (Hz) of the emitted spectrum is calculated from the measured power spectrum  $P(\nu)$ .

See section 2.7

### 2.3.2.d. Pulse repetition rate

The emitted optical pulse repetition rate,  $f_{pulse}$ , (as opposed to the laser trigger signal frequency  $f_{clock}$ ) must be confirmed by measurement.

For a QKD transmitter  $f_{pulse}$  is expected to be double the laser optical output rate  $f_{clock}$  because of the embedded AMZI.

See Section 2.2 for measurement details.

### 2.3.2.e. Measurement of emitted pulses

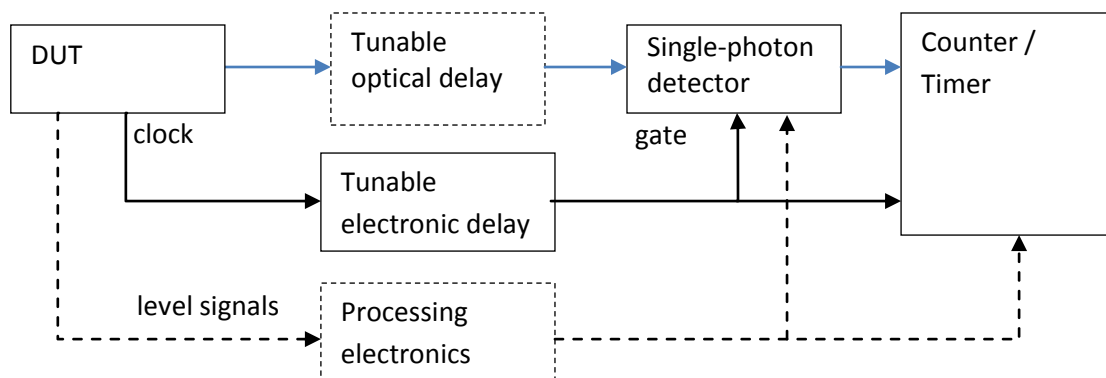


Figure 2.2 Experimental set-up

The set-up shown in Figure 2.2 is used to measure the emitted pulses. Blue lines indicate optical signals, black lines electrical signals.

If the normal operation of the DUT is that it provides the master clock, then the system as shown in Figure 2.2 should be used.

If the normal operation of the DUT is that another device (e.g. the QKD receiver) provides the master clock, then the system as shown in Figure 2.2 should be adapted, with the other device providing the master clock to the DUT and tunable electronic delay.

Using a tunable electronic or optical delay, or both, the arrival of photons is set within the optical gate of the detector.

The detector gate frequency is either the same as the clock frequency, or an integer sub-multiple of the clock frequency. In the latter case, a frequency divider can be included in the electronic delay circuit.

The time between successive detector gates must exceed the detector dead-time, and ideally, the detector recovery time.

In the case of (c), additional signals may need to be processed to identify the random changes in mean photon number settings (see dotted lines figure 2.2).

For incident photons from a specific mean photon number setting, the number of illuminated detector gates,  $N_{gates}$ , and the corresponding number of detections,  $N_{det}$ , is recorded.

### 2.3.2.f. Calculation

The detection probability  $p^{det}$  for a pulse for a specific mean photon level setting is recorded, where

$$p^{det} = \frac{N_{det}}{N_{gates}}, \quad (2.3)$$

with  $N_{det}$ : number of detections in  $N_{gates}$ ,  $N_{gates}$ : number of illuminated gates.

The number of detections  $N_{det}$  contains also dark counts and after-pulses:

$$N_{dark} = N_{gates} p^{dc} \quad (2.4)$$

$$N_{after} = (N_{true} + N_{dark}) p^{after} \quad (2.5)$$

where

$p^{dc}$ : dark count probability;

$N_{dark}$ : number of dark counts;

$p^{after}$ : after-pulse probability;

$N_{after}$ : number of afterpulses;

$N_{true}$ : number of true photon events.

The mean photon number is given by (see Appendix 2):

$$\mu = \frac{1}{\eta} \ln \left( 1 - \frac{N_{true}}{N_{gates}} \right) = \frac{1}{\eta_D} \ln \left\{ 1 - \frac{p^{det}}{1 + p^{after}} + p^{dc} \right\} \quad (2.6)$$

where  $\eta$  is the detection efficiency of the photon counter.

The value of  $\eta$  may need to be adjusted if:

- (i) the spectrum of the emitted pulses is different to the wavelength at which the detector was calibrated. In this case an estimate of the detection efficiency of the photon counter at the emitted wavelength must be made;
- (ii) the temporal extent of the emitted pulses are different to that used to calibrate the photon counter; see [24].

Additional corrections may be needed to take account of detector recovery efficiency.

## **2.4 Mean power of pulses emitted by QKD transmitter**

These guidelines cover the measurement of the mean output power of the pulses emitted by a fibre-coupled Device Under Test (DUT) operating in the following modes:

- (a) The DUT emits pulses with the same  $\mu$ ;
- (b) The DUT emits pulses whose  $\mu$  changes according to a fixed, repetitive pattern;
- (c) The DUT emits pulses whose  $\mu$  changes randomly from pulse to pulse.

### **2.4.1 Direct measurement with a calibrated power meter**

- (a) The emitted power from the DUT is high enough to be measurable with a power meter
- (b) The sensitivity of the power meter is such that the power cannot be measured at the single-photon output of the DUT. In this case, arrangements must be made to measure the optical pulses before they are attenuated to the single-photon level, and the transmittance from the point of measurement to the exit of the DUT must also be measured.

Where the DUT is a QKD transmitter, this method only allows the mean power, averaged over all emitted pulses of emitted mean photon numbers, to be measured.

#### **2.4.1.a Required equipment**

- (i) Fibre-coupled power meter

The optical power responsivity must be traceably calibrated to the SI at the repetition rate of the DUT pulses, and in the spectral region of interest

#### **2.4.1.b Power**

The power meter (the optical measurement device in figure 2.1) is now connected to the DUT.

The emitted power is measured using the power meter, and corrected for any signal offset in the absence of radiation.

The corrected value, averaged over the required time-interval, is given by  $\langle P_{meas} \rangle$  (W)

### 2.4.1.c Calculation

The mean power is then given by

$$\langle P \rangle = \langle P_{meas} \rangle t \quad (2.7)$$

where  $t$  is the transmittance of the path from the actual measurement position to the desired measurement position.

### 2.4.2 Measurement of $\mu$

The mean photon numbers are continuously measured, using the methods described in section 2.3.2, during the key session, and their mean values, averaged over a key session or other time-interval, obtained.

$$\langle P \rangle = \left\langle \left( \sum_1^{2n} \mu_j p_j \right) \right\rangle f_{pulse} h \nu_m \quad (2.8)$$

where

$n$  is the number of different decoy states measured

$\mu_j$  are the measured mean photon numbers (one for each arm of the AMZI per decoy state)

$p_j$  are the relative fractions of the total number of pulses emitted by each  $\mu_j$

$f_{pulse}$  is the total pulse output rate (Hz)

$h$  is Planck's constant

$\nu_m$  is the mean frequency of the pulses (assumed to be identical)

## 2.5 Source power stability

These guidelines cover the measurement of the mean output power of the pulses emitted by a fibre-coupled Device Under Test (DUT) operating in the following modes:

- (a) The DUT emits pulses with the same  $\mu$ ;
- (b) The DUT emits pulses whose  $\mu$  changes according to a fixed, repetitive pattern;
- (c) The DUT emits pulses whose  $\mu$  changes randomly from pulse to pulse.

Measurements can be carried out as described in sections 2.4.1 or 2.4.2, where the time of each measurement period is suitably short so that the variation of the output power can be recorded, and the stability determined.

The span and standard deviation of the frequency histogram of the output power gives the peak-to-peak and standard deviation of the variation in output power.

## 2.6 Source timing jitter

Measurement can be carried out with a single-photon counter after attenuation to the single-photon level, or with a fast photodiode before attenuation to the single-photon level.

Superconducting nanowire single-photon detectors (SNSPDs) exhibit the lowest jitter ( $< 100$  ps) of single-photon detectors, [19,25,26], and are commercially available. In addition, the jitter profile tends to be Gaussian-shaped, which facilitates deconvolution.

Measurement prior to the attenuator that reduces the flux to the single-photon level can be carried out with a fast photodiode, which has a higher bandwidth and significantly less jitter than an SNSPD.

### 2.6.1 Measurement at single-photon level

The measurement set-up is shown in figure 2.3

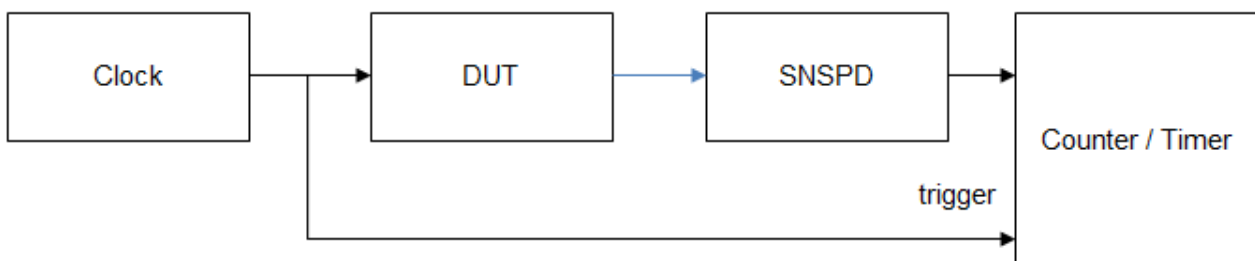


Figure 2.3 Experimental set-up

#### 2.6.1.a Required equipment

- (i) Master clock.

This could be an external device, or an internal clock within the DUT which is used to drive the laser, and which is also accessible to trigger the counter/timer.

- (ii) Fibre-coupled SNSPD (continuously-gated, non-photon-number-resolving).

The temporal response profile of the detector must have been previously measured (see section 3.10)

(ii) Counter/timer

The timer/counter should be able to generate histograms of recorded events as a function of time relative to the trigger pulses, or provide raw data from which such histograms can be generated. The temporal resolution of the timer/counter should be such that the observed full-width at half-maximum (FWHM) of the histogram spans a minimum of 10 time bins.

### 2.6.1.b Measurement

A histogram of detection times will be observed by correlating many successive detection events with the clock signal triggering the source. This histogram is the temporal response profile due to the source emission temporal profile, the detector signal jitter, and any jitter due to the timer/counter (assumed to be negligible).

### 2.6.1.c Calculation

The detector's intrinsic response profile is deconvolved from the measured signal, which yields the source emission temporal profile. This is due to the jitter of the laser output with respect to the input trigger signal, plus the natural temporal linewidth of the laser emission.

The span and standard deviation of the histogram gives the peak-to-peak and standard deviation jitter.

When measuring the jitter of a single-photon signal using an SNSPD, a measurement uncertainty of  $< 50$  ps is feasible.

## 2.6.2 Measurement prior to attenuation to single-photon level

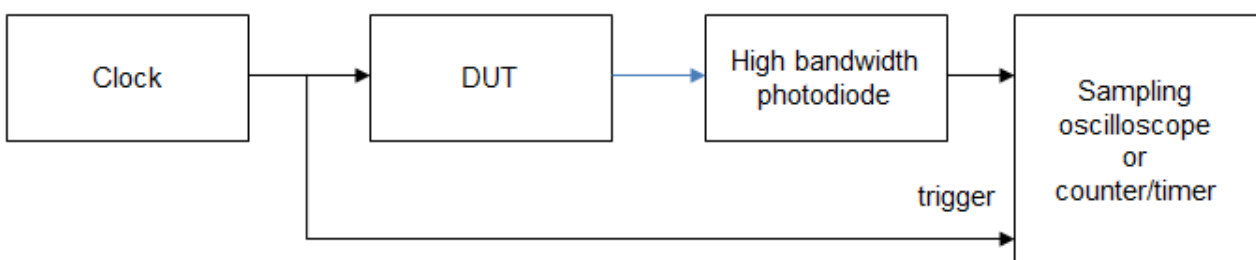


Figure 2.4 Experimental set-up

### 2.6.2.a Required equipment

- (i) Master clock.

This could be an external device, or an internal clock within the DUT which is used to drive the laser, and which is also accessible to trigger the counter/timer.

- (ii) High-bandwidth photodiode
- (iii) High-bandwidth sampling oscilloscope, or
- (iii) Counter/timer

The timer/counter should be able to generate histograms of recorded events as a function of time relative to the trigger pulses, or provide raw data from which such histograms can be generated. The temporal resolution of the timer/counter should be such that the observed full-width at half-maximum (FWHM) of the histogram spans a minimum of 10 time intervals.

#### **2.6.2.b.1 Measurement with oscilloscope**

The oscilloscope is set to a mode such that a histogram of sampled points from the trace produced by the photodiode, as a function of time relative to the trigger, is accumulated.

##### **2.6.2.c.1 Calculation**

The baseline and maximum of the observed histogram is estimated.

A histogram of the number of points (as a function of time) on the rising edge of the histogram at the half-height value is calculated. This histogram is the temporal response profile due to the source emission temporal profile, detector signal jitter and scope jitter. In practice, the detector and scope jitter are likely to be negligible. The span and standard deviation of this histogram gives the peak-to-peak and standard deviation jitter for the rising edge of the pulse.

A histogram of the number of points (as a function of time) on the falling edge of the histogram at the half-height value is calculated. This histogram is the temporal response profile due to the source emission temporal profile, detector signal jitter and scope jitter. In practice, the detector and scope jitter are likely to be negligible. The span and standard deviation of this histogram gives the peak-to-peak and standard deviation jitter for the falling edge of the pulse.

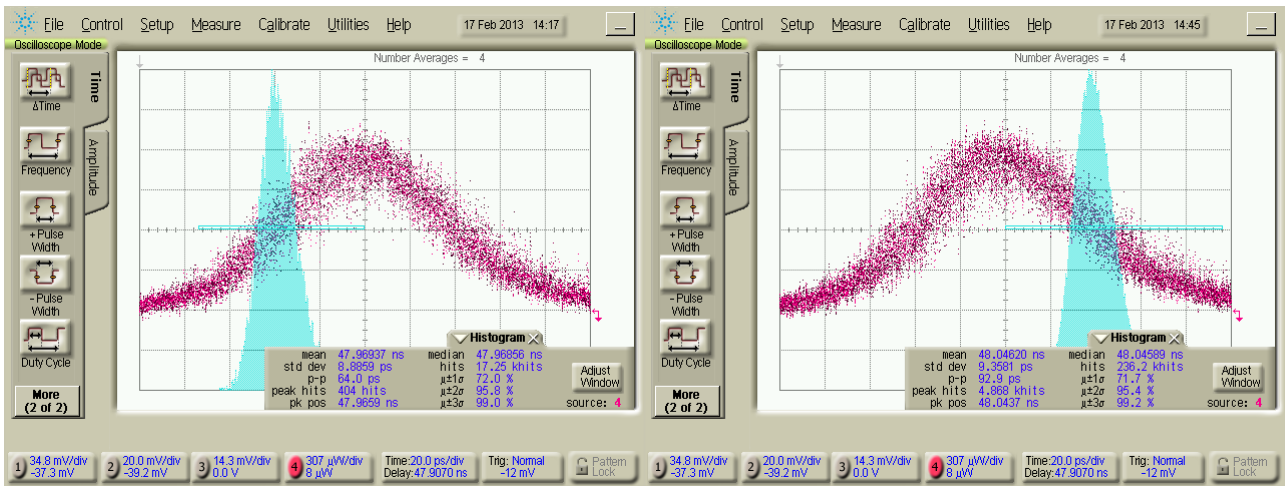


Figure 2.5. Examples of analysis of rising and falling edge of measured pulse. The blue rectangles denote the region over which the histograms are calculated. The jitter of the rising edge (8.9 ps) is less than that of the falling edge (9.4 ps).

### 2.6.2.b.2 Measurement with counter/timer

A histogram of detection times will be observed by correlating many successive detection events with the clock signal triggering the source. The height of the photodiode signal can be established by varying the threshold setting for the signal from the photodiode. The threshold is then set to the half-height for a rising edge, and a histogram of the number of points (as a function of time) is obtained. The threshold is then set to the half-height for a falling edge, and a histogram of the number of points (as a function of time) is obtained. These histograms are the temporal response profile due to the source emission temporal profile, the detector signal jitter, and jitter due to the timer/counter.

#### 2.6.2.c.2 Calculation

In practice, the jitter due to the detector and counter/timer is likely to be negligible.

The span and standard deviation of the rising edge histogram gives the peak-to-peak and standard deviation jitter for the rising edge of the pulse.

The span and standard deviation of the falling edge histogram gives the peak-to-peak and standard deviation jitter for the falling edge of the pulse.

## 2.7 Source wavelength

### 2.7.a Equipment required

(i) Fibre-coupled spectrometer

This encompasses all devices capable of measuring the spectrum of the emitted pulses, and includes wavemeters, optical spectrum analysers, etc.

The spectral range of sensitivity should cover the entire spectral region over which emission occurs. When the laser in the QKD source is driven to emit short optical pulses, typically  $< 100$  ps in duration, the spectral width of the source,  $\Delta\nu_{\text{source}}$ , will be greater than 10 GHz (0.08 nm), but is more likely to be of the order of 120 GHz (1 nm).

The frequency or wavelength scale of the spectrometer must be calibrated traceably to the SI.

The linearity of the intensity axis should be calibrated.

(ii) Tunable delay

A means (such as a tunable delay) for synchronising the arrival of a pulse or photon at the detector within the detection window or detector gate.

(iii) Counter/timer

The timer/counter should be able to generate histograms of recorded events as a function of time relative to the trigger pulses, or provide raw data from which such histograms can be generated. The temporal resolution of the timer/counter should be such that the observed full-width at half-maximum (FWHM) of the histogram spans a minimum of 10 time bins.

## 2.7.b Measurement

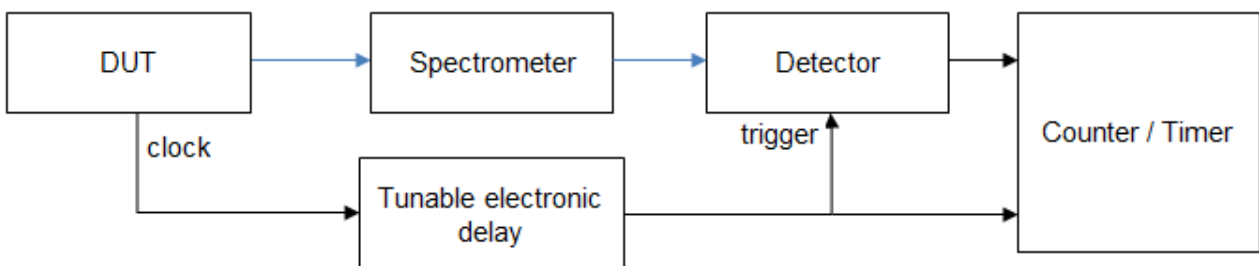


*Figure 2.6 Experimental set-up.*

The experimental set-up is shown in Figure 2.6, or a variant thereof. The detector may be integral to the spectrometer, or separate from it.

If the sensitivity of the spectrometer/detector combination is such that the spectrum cannot be measured at the single-photon output of the DUT, arrangements must be made to measure the optical pulses before they are attenuated to the single-photon level.

It is assumed that the spectrum is measured spectral point by spectral point. The electronic delay ensures that a measurement is carried out such that the emission from the DUT is synchronised to the detector measurement window.

Where measurements are carried out at the single-photon level, the same considerations as in sections 2.3.2.a, 2.3.2.b, 2.3.2.d and 2.3.2.e apply.

The spectrum  $P(\nu)$   $\text{W}\cdot\text{Hz}^{-1}$  of the emitted pulses is measured, or calculated from measured  $P(\lambda)$   $\text{W}\cdot\mu\text{m}^{-1}$

### 2.7.c Calculation

The source wavelength can be taken as either the frequency or wavelength of peak emission, or the mean frequency or wavelength of the emission.

The mean spectral frequency  $\nu_m$  (Hz) of the emitted spectrum is calculated from  $P(\nu)$ :

$$\nu_m = \frac{\sum_1^n w_i P(\nu)_i}{\sum_1^n w_i} \quad (2.9)$$

where  $w_i$  represents the spectral width of the respective measured power value  $P(\nu)_i$ .

If the spectrum was measured at a point before the desired measurement position, the spectrum must first be multiplied by the spectral transmittance  $t(\nu)$  of the path from the actual measurement position to the desired measurement position, before calculating its mean spectral frequency  $\nu_m$ .

## 2.8 Spectral linewidth

The spectrum of the emitted pulses is measured as described in Section 2.7

The linewidth is normally defined as the full width at half-maximum (FWHM) of the measured spectral profile.

## 2.9 Spectral indistinguishability

For evaluating spectral indistinguishability, the parameter  $x$  in equations A4.1 & A.4.2 (see Appendix 4) is frequency  $\nu$  (or wavelength  $\lambda$ ).

The set-up is as shown in figure 2.7, or a variant thereof. Measurements may be carried out using a fixed pattern of phase settings, or a random pattern as used in QKD.

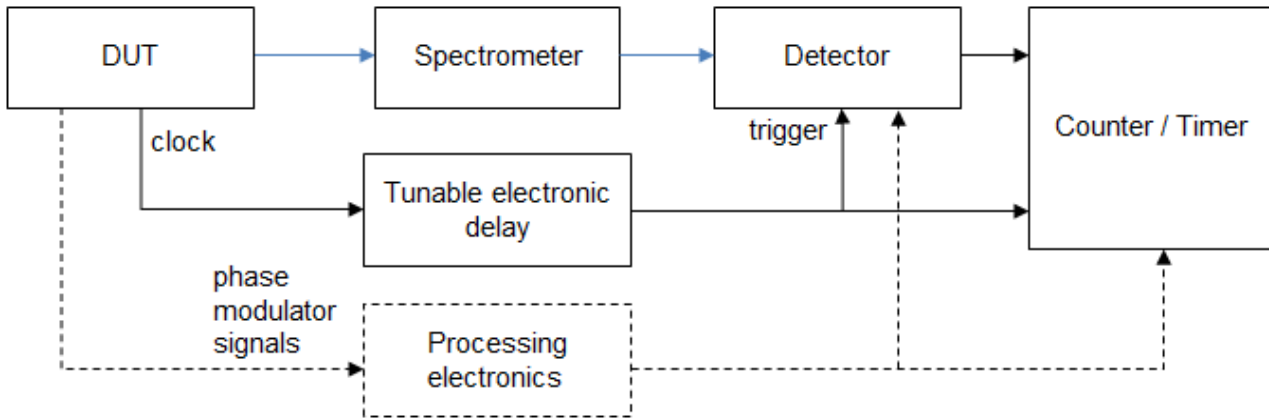


Figure 2.7 Experimental set-up

### 2.9.a Required equipment

#### (i) Fibre-coupled spectrometer

This encompasses all devices capable of measuring the spectrum of the emitted pulses, and includes wavemeters, optical spectrum analysers, etc.

The spectral range of sensitivity should cover the entire spectral region over which emission occurs. When the laser in the QKD source is driven to emit short optical pulses, typically  $< 100$  ps in duration, the spectral width of the source,  $\Delta\nu_{\text{source}}$ , will be greater than 10 GHz (0.08 nm), but is more likely to be of the order of 120 GHz (1 nm).

The frequency or wavelength scale of the spectrometer must be calibrated traceably to the SI.

The linearity of the intensity axis should be calibrated.

#### (ii) Tunable delay

A means (such as a tunable delay) for synchronising the arrival of a pulse or photon at the detector within the detection window or detector gate.

#### (iii) Counter/timer

The timer/counter should be able to generate histograms of recorded events as a function of time relative to the trigger pulses, or provide raw data from which such histograms can be generated. The temporal resolution of the timer/counter should be such that the observed full-width at half-maximum (FWHM) of the histogram spans a minimum of 10 time bins.

(iv) Signal-processing electronics

Where a random pattern of phases is generated, additional signals may need to be processed to identify selected phase transitions (dotted lines in figure 2.7).

## 2.9.b Measurement

The spectrum of the transmitted pulses is measured as described in Section 2.7.

Measurements can be carried out either before signals are attenuated to the single-photon level, or after attenuation to the single-photon level.

It is assumed that the spectrum is measured spectral point by spectral point. The electronic delay ensures that a measurement is carried out such that the emission from the DUT is synchronised to the detector measurement window.

Where measurements are carried out at the single-photon level, the same considerations as in sections 2.3.2.a, 2.3.2.b, 2.3.2.d and 2.3.2.e apply.

The spectral profile of the photons can be acquired for each of the four encoding phases while the phase remains constant. These reference spectral profiles should be compared to those acquired when the encoding phase is switched prior to the laser pulse propagating through the modulator (as in the normal operation of the QKD transmitter). Any difference between these spectral profiles constitutes a spectral distinguishability. Note that the spectral resolution of the measuring device must be adequate to resolve spectral features.

### 2.9.b.1 Fixed phase pattern

A cyclic 12-element phase pattern can be used, which provides all twelve phase transitions possible for the BB84 protocol. This covers the eventuality that the previous phase setting of the modulator may affect the timing of the subsequent phase setting.

If a gated detector is used, by delaying the gate triggers in increments of one clock period, the spectra of pulses following all 12 phase transitions can be measured. If the detector attached to the spectrometer (measurements at single-photon level) has to be gated at a lower frequency than the transmitter clock frequency, the simple example pattern shown in figure 2.8 will need to be

adjusted.

If a continuously gated detector (high power regime, or single-photon level) is used, a timer/counter can be repeatedly triggered at the same point in a cycle, and data then accumulated over many cycles.

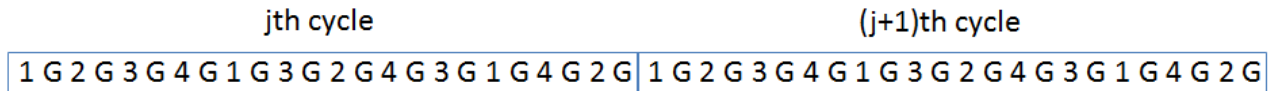


Figure 2.8. Example of a cyclic phase pattern used which encompasses all 12 phase transitions. Numerals indicated phase settings, G indicates detector gates.

### 2.9.b.2 Random phase pattern

Where a random pattern of phases is generated, additional signals may need to be processed to identify selected phase transitions (see dotted lines in figure 2.7).

### 2.9.c Calculation

The parameter  $S_{AB}^{ind}$ , which represents the indistinguishability in the spectrum in phase state  $B$  with respect to the spectrum of phase state  $A$ , where state  $B$  follows state  $A$ , is given by Eqn. 4.2, where  $x = \nu$  (or  $\lambda$ ).

## 2.10 Temporal profile

Measurement must be carried out with a fast photodiode before attenuation to the single-photon level, and is similar to that used to measure jitter (Section 2.6)

Measurement at the single-photon level is limited by the fact that the narrowest single-photon detection profile currently obtainable is from SNSPDs which exhibit a jitter of 50-100 ps (see section 2.6). A measurement can be carried out with a triggerable detector, where detector counts can be measured as the detector gate is swept through the laser pulse (or vice-versa), and the data plotted as function of time delay between the detector trigger and the laser trigger. The previously established detector profile (Section 3.1) can then be deconvoluted from the resulting curve (the synchronisation curve) to yield the pulse temporal profile.

Measurement with a continuously gated detector will be complicated by the non-zero dead time of the detector, i.e. detections after the beginning of the pulse will be depressed due to the dead time incurred by detections in the earlier part of the pulse.

### 2.10.a Required equipment

- (i) Master clock.

If the DUT provides its own clock signal for driving the laser, and this signal is accessible, this signal can be used to trigger the counter/timer.

- (ii) High-bandwidth photodiode
- (iii) High-bandwidth sampling oscilloscope, or
  - (v) Counter/timer

The timer/counter should be able to generate histograms of recorded events as a function of time relative to the trigger pulses, or provide raw data from which such histograms can be generated. The temporal resolution of the timer/counter should be such that the observed full-width at half-maximum (FWHM) of the histogram spans a minimum of 10 time bins.

### **2.10.b Measurement with oscilloscope**

The oscilloscope is set to a mode such that a histogram of sampled points from the trace produced by the photodiode, as a function of time relative to the trigger, is accumulated.

The mean signal level for each time-delay is then calculated to obtain the resulting response curve.

### **2.10.c Measurement with counter/timer**

A histogram of detection times will be observed by correlating many successive detection events with the clock signal triggering the source. Data will be collected as the threshold setting for the signal from the photodiode is varied from ground up to the maximum value of the photodiode signal (rising edge trigger) and then as the threshold setting is reduced back down to ground (falling edge trigger).

The mean time for each detection level is calculated, and the resulting data plotted as signal level versus time delay from the trigger to obtain the response curve.

### **2.10.d Calculation**

The obtained response curve is the temporal response profile due to the source emission temporal profile as well as detector and oscilloscope or counter/timer jitter. The detector, oscilloscope and counter/timer jitters are likely to be negligible, and this curve can be taken to represent the source temporal profile. If the FWHM of the response curve is less than five times broader than the FWHM of the detector response profile, one may wish to consider deconvolving the detector response curve from the temporal response profile.

Where both profiles are symmetric, and similar to Gaussian profiles, the following calculation can

be applied:

$$FWHM_{source}^2 = FWHM_{response}^2 - FWHM_{response}^2 \quad (2.9)$$

## 2.11 Temporal indistinguishability

For evaluating spectral indistinguishability, the parameter  $x$  in equations A4.1 & A.4.2 (see Appendix 4) is time  $t$ .

Measurements of the temporal profile of the emitted pulses are coarried out as described in Section 2.10, for all pair combinations of intensity settings, all pair combinations of phase settings (Section 2.9).

The parameter  $T_{AB}^{ind}$ , which represents the indistinguishability in the temporal profile in state  $B$  with respect to the temporal profile of state  $A$ , where state  $B$  follows state  $A$ , is given by Eqn. 4.2, where  $x = t$ . States  $A, B$  may be intensity states (as used in decoy protocols), or phase states.

## 2.12 Single-photon emission efficiency (Grangier parameters and pulse-to-pulse stability)

For a real (practical) single-photon source (SPS) the most important characterization consists in verifying the possibility of having more than one photon emitted by the source. The most common set-up used for this is the Hanbury Brown-Twiss interferometer (HBT) operating at single photon level.

### 2.12.a Equipment required

An HBT interferometer composed of

- a 50:50 Beam-Splitter (pigtailed)
- two single-photon detectors (click/no-click, fiber-coupled)
- time-tagging or coincidence electronics, and counters

### 2.12.b Measurement

The HBT is implemented by placing a threshold (click/noclick) detector at each of the output ports of a 50:50 beam-splitter.

The efficiency of a single-photon source can be described by means of the parameter  $\alpha$  proposed by Grangier et al. [27]:  $\alpha = Q(2)/[Q^{(I)}(1) Q^{(II)}(1)]$ ; where  $Q(2)$  is the probability of a coincidence of clicks from the two detectors, while  $Q(1)$  is the probability of a click by each detector, and (I), (II) respectively indicate the detector placed at the transmission and reflection ports of the beam splitter. These probabilities should be evaluated as relative frequencies of counted events.

The probabilities  $Q$  are evaluated as the ratio between the counts (coincident counts between the two detectors in the case of  $Q(2)$ , counts of each single detector in the case of  $Q(1)$ ), and the number of gates.

It is worth noting that with typical click-no-click detectors the  $\alpha$  parameter is (almost) independent of the detection efficiency of the detectors (when very similar between the two detectors), while it can be strongly affected by the presence of dark counts or counts due to stray-light. For this reason time-correlated-photon-counting measurement techniques can be helpful to provide proper estimation of the background counts. Furthermore, detector deadtime and HBT interferometer beam-splitter imbalance may bias the estimation of  $\alpha$ . Proper estimation of these non-idealities are necessary to implement the needed corrections factor required for a faithful estimation of  $\alpha$  [17].

Despite being apparently not useful in the case of an SPS based on an attenuated laser (since the  $\alpha$  parameter should be equal to one, a value that is independent of the intensity of the coherent source), its estimation is important since it provides information about the pulse-to-pulse stability of the attenuated laser output, in fact pulse instabilities result in a super-Poissonian behaviour of the laser. Such instabilities may open a security leakage in QKD systems since they may correspond to the number of pulses containing photons being different to the one predicted by the theoretical Poissonian distribution.

## **2.13 Polarisation state**

Photon polarisation is the quantum mechanical equivalent of the classical electromagnetic light polarisation. The quantum polarisation state vector for a single photon, for instance, is identical with the Jones vector, usually used to describe the polarisation of a classical wave. Thus, quantum state tomography is equivalent to the estimation of the four Stokes parameters for classical light, with the only difference being: instead of measuring light power, what is experimentally observed are the relative detection frequencies of single photon detection, i.e. conditional probabilities of detection of single photons. Tomographic reconstruction of the polarization state at the single photon level is more affected by detection imperfections (dark counts, afterpulses, etc) than conventional polarimetry employing well-established light detection technology in the macroscopic regime. For this reason, proper reconstruction algorithms (e.g. maximum-likelihood) should be employed to reconstruct physically meaningful polarisation state information about the single photons.

### **2.13.a Equipment required**

A single photon polarimeter usually composed of

- a polarising Beam-Splitter
- a quarter-wave and a half-wave plate
- two single-photon click/no-click detectors
- time-tagging or coincidence electronics, and counters

### **2.13.b Measurement**

The Stokes parameters, in the case of the polarisation state reconstruction of single-photons, are obtained from a set of four measurements, corresponding to four different polarisation projections. These parameters, which fully characterize the polarization state of the light, are related to the number of photons registered by the detector after each of the four measurements. It is therefore

possible to reconstruct the density matrix associated to the quantum state, and this reconstruction is usually referred to as Quantum State Tomography (QST).

The simplest QST consists of measuring the number of photons with the following single photon detector measurements: with no polariser  $n_0$  (or in any arbitrary polarisation summing up the counts of the two detectors, this is essentially the normalisation condition); with a polarizer that transmits only horizontally  $\langle H \rangle$  polarized light  $n_1$ ; with a polarizer that transmits only light diagonally  $\langle D \rangle$  polarized at  $45^\circ$  with respect to the horizontal  $n_2$ ; and with a polarizer that transmits only right-circularly polarized  $\langle R \rangle$  light  $n_3$ .

The way to perform an arbitrary projective measurement exploits a half-wave plate and a quarter-wave plate, followed by a polarizing beam splitter that separates horizontal and vertical components of polarization. The Stokes parameters, which fully characterize the polarization state of the light, are defined through the measurement of  $n_0, n_1, n_2, n_3$ :  $S_0 = n_0$ ,  $S_1 = (2 n_1 - n_0)$ ,  $S_2 = (2 n_2 - n_0)$ ,  $S_3 = (2 n_3 - n_0)$ .

### 2.13.c Calculation

Any single qubit density matrix  $\rho$  can be uniquely represented by the four Stokes parameters according to the formula:

$$\rho = \frac{1}{2} \sum_{i=0}^3 \frac{S_i}{S_0} \sigma_i \quad (2.10)$$

where  $\sigma_i$  are the Pauli matrices (and  $\sigma_0 = 1$ ).

Usually, the density matrix reconstructed by direct inversion of the above equation is inaccurate and often unphysical. This is due to experimental inaccuracies and statistical fluctuations of photon counts. To avoid this problem, maximum-likelihood estimation or other optimization techniques are usually employed, but these algorithmic approaches do not provide a reliable estimation of the uncertainty.

### 3. Single-photon detector characterisation

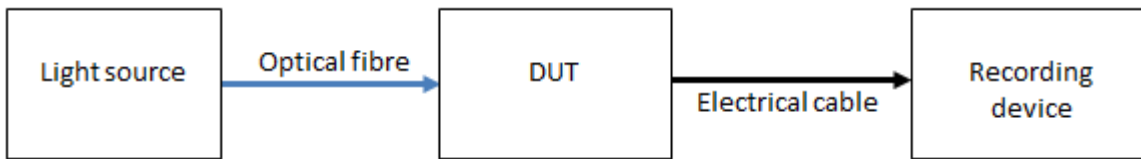


Figure 3.1 Generic experimental set-up

Figure 3.1 illustrates the generic experimental set-up for measuring a single-photon detector. A light source, such as an attenuated pulsed laser capable of producing a stream of photons, is sent to the DUT via an optical fibre, and the DUT response is sent to a recording device.

#### 3.1 Clock frequency

The frequency of the clock signal,  $f_{clock}$ , used to gate the single-photon detector(s) in the receiver can be measured using standard traceable time and frequency calibration techniques – i.e. by measuring the pulse train with a high bandwidth oscilloscope.

##### 2.1.a Equipment required

- (i) High-bandwidth oscilloscope

This instrument must be capable of temporally resolving the signal emitted by the clock..

#### 3.2 Detector gate repetition rate

The actual gate repetition rate,  $f_{gate}$ , (as opposed to the clock trigger signal frequency  $f_{clock}$ ) must be confirmed by measurement.

#### 3.3 Detector gate detection probability profile

The set-up is as shown as in figure 3.1.

##### 3.3.a. Required equipment

- (i) CW laser operating at wavelength for which calibration is required.
- (ii) Timer/counter capable of recording events as a function of time from an input trigger.

##### 3.1.b. Measurement

The measurement is based on the fact that photons from a CW laser are created at random points in time, and over many events yield a uniform time distribution.

The timer/counter is triggered every  $R$ th gate, where  $R$  is an integer ( $\geq 1$ ), and a histogram of detections versus time after the trigger is accumulated. This histogram will yield the relative temporal profile of the detector gate detection probability.

### **3.1.c Calculation of detection probability profile?**

The relative detection probability profile might be convertible into a detection efficiency profile if the detection probabilities could be made absolute.

## **3.4 Dark count probability (per gate)**

The set-up is as shown as in figure 3.1, except that no light probe is required, since no light is to be sent to the DUT.

### **3.4.a Required equipment**

- (i) Pulse-counter used as recording device.

### **3.4.b Measurement**

The detector is gated as a set frequency  $f_{gate}$ , and gate duration  $t_{gate}$ .

The optical input to the DUT is blocked, and the number of counts per second,  $N$ , from the pulse-counter is recorded.

### **3.4.c Calculation**

The dark count probability per gate of duration  $t_{gate}$ ,  $P_{dark}$ , is given by

$$P_{dark} = \frac{N}{f_{gate}} \quad (3.1)$$

## **3.5 After-pulse probability**

The after-pulse probability and detector efficiency are measured using the same set-up. The basic principle is that the laser pulse frequency  $f_{source}$  is stepped down by an integer factor  $R$  compared to the detector gate rate using a frequency divider. Therefore, only every  $R$ th detector gate will be

illuminated. Counts in the unilluminated gates will be solely due to dark counts and after-pulses, while counts in the illuminated gates will be due to true detections, after-pulses, and detections [20].

### **3.5.a Required equipment (all fibre-coupled)**

#### **(i) Pulse generator**

Required to trigger the detector gates. If the detector generates its own gate trigger signal, and this can also be accessed externally, then this item is not required. In what follows below, it is assumed that the gate trigger signal is either derived from the DUT, or an external pulse generator.

#### **(ii) Pulsed laser**

The laser should operate at the wavelength for which the detection efficiency is required to be measured. The duration of the output pulses must be narrower than the duration of the detector gate (see sections 2.10 and 3.1), the narrower the better.

In principle, a CW laser, combined with a means for carving out pulses from this CW output, such as an intensity modulator, can also be used. The duration of these pulses must be narrower than the duration of the detector gate, the narrower the better. Hence, an equal duty cycle modulation signal will not be appropriate. Very good extinction is required to minimise emission outside of the pulses so that mean photon number can be reliably estimated from measurement of the optical power.

The pulsed laser, or the intensity modulator, must be capable of being driven by an external clock signal.

#### **(iii) Spectrometer**

Fibre-coupled spectrometer for measuring the spectrum of the emitted pulses – this encompasses all devices capable of measuring the spectrum of the emitted pulses, and includes wavemeters, optical spectrum analysers, etc.

The spectral range of sensitivity should cover the entire spectral region over which emission occurs.

The frequency or wavelength scale of the spectrometer must be calibrated traceably to the SI.

The linearity of the intensity axis should be calibrated

#### **(iv) Frequency divider**

The frequency divider is used to reduce the frequency of the detector gate trigger signal by an integer factor  $R$ . This signal is then used to drive the pulsed laser.

(v) Two-channel waveform or function generator\*

An alternative to using a frequency divider is to replace the pulse generator and frequency divider by a two-channel waveform or function generator capable of providing two synchronised signals to trigger the detector gates and the laser. This functionality will be required for measuring dead time and recovery time (Sections 3.6 to 3.8)

(vi) Variable delay line

The variable delay line is used to vary the time delay between the signal used to trigger the detector and the signal used to trigger the laser, in order to synchronise the arrival of the laser pulse within a detector gate. Any jitter introduced by the delay line should not lead to any photons arriving at the detector outside the duration of its gate.

(vii) Calibrated optical attenuator

A calibrated optical attenuator is required to attenuate optical pulses, from the level at which they can be measured with a power meter, to the single photon level. If a calibrated optical attenuator is not available, it can be calibrated using a calibrated power meter – e.g. see [24]

(viii) Second optical attenuator (does not need to be calibrated)

This attenuator is required to attenuate the pulses output from the laser to a value that: (a) can be measured with the power meter; (b) is sufficiently low so that the calibrated attenuator can then attenuate the resulting optical pulses to the single-photon level. This item is not required if the calibrated optical attenuator (vii) has sufficient dynamic range to implement (a) and (b).

(ix) Calibrated optical power meter\*

The optical power responsivity must be traceably calibrated to the SI at the repetition rate of the DUT pulses, and in the spectral region of interest.

\*Note that this item is not strictly required for measurement of after-pulse probability, but it is required for measurement of detection efficiency (Section 3.4). However, it is useful to use this item to check the mean photon number of the pulses sent to the DUT.

(x) Counter/timer

The counter/timer must be capable of operating in multi-stop mode with dead time less than the time between consecutive detector gates. The device should be able to

generate time histograms of recorded events, or provide raw data from which such histograms can be generated.

### 3.5.b Measurement

The mean spectral frequency  $\nu_m$  (Hz) of the pulses emitted by the laser is obtained as described in Section 2.7.

The dark count probability will be required (Section 3.2)

The following set-up (or variants thereof) can then be used to measure after-pulse probability (and detection efficiency).

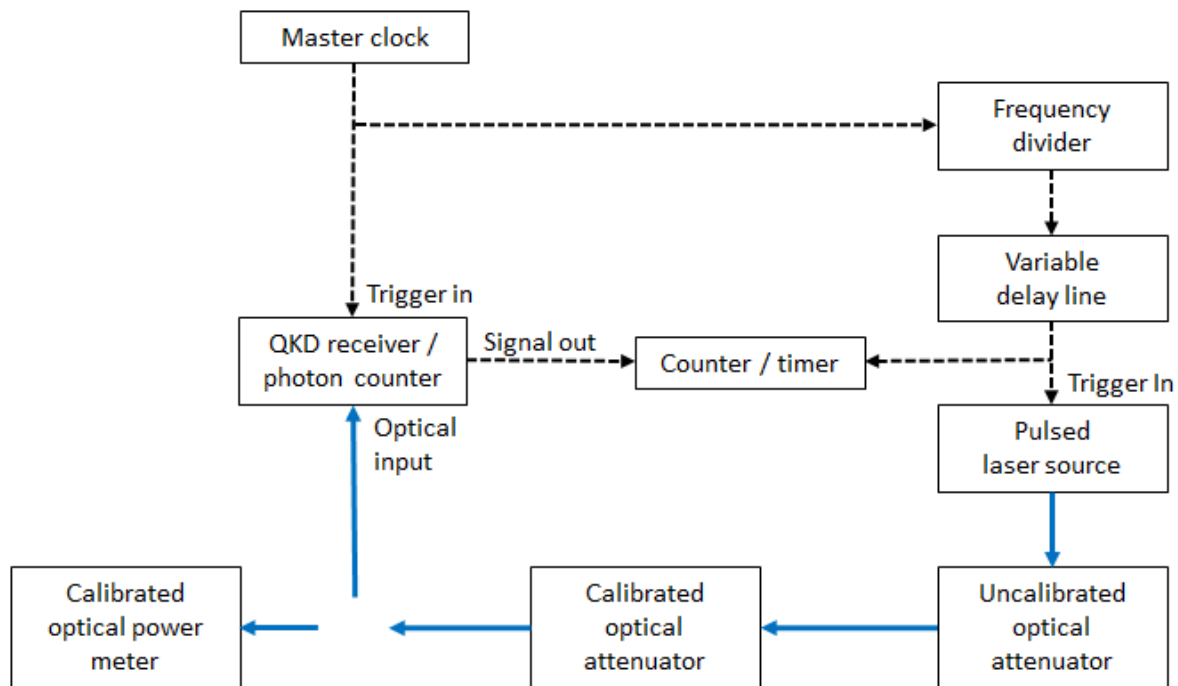


**Figure 3.2.** Set-up for calibration of QKD photon counter(s). Electronic connections are shown in dashed lines, fibre-optic connections in solid lines. The output of the calibrated optical attenuator can be connected to either the calibrated power meter or the QKD receiver/photon counter. The master clock may be part of the QKD receiver.[24]

The laser pulse frequency  $f_{source}$  is stepped down by an integer factor  $R$  compared to the detector gate rate  $f_{gate}$  using a frequency divider. Therefore, only every  $R$ th detector gate will be illuminated.

The output of the pulsed laser is transmitted through an (uncalibrated) attenuator and a calibrated attenuator and measured with the calibrated optical power meter. The calibrated attenuator is set to its lowest attenuation setting,  $A_{low}$  (dB), that encompasses its insertion loss, and the uncalibrated attenuator is used to reduce the optical power from the laser to a value that: (i) can be measured with the power meter; (ii) is sufficiently low so that the calibrated attenuator can then attenuate the resulting optical pulses to the single-photon level. The power  $P_A$  is measured with the power meter. [In principle, the optical power measurement may be carried out for  $f_{source} \geq f_{gate}$ , and then  $f_{source}$  reduced to  $f_{gate}/R$  for the DUT measurements. In this case, one needs to confirm that the optical pulses are independent of the repetition rate (and any changes to the electrical trigger pulses that the frequency divider may generate)].

The attenuation of the calibrated attenuator is then increased to  $A_{hi}$  (dB) so that the output pulses are reduced to the single-photon level, and sent to the DUT. The arrival of the laser pulses at the detector is synchronised to occur within the detector gates using the low-jitter delay line. The shape of the detector gate efficiency can be used to determine when the pulse is centred on the gate, but synchronisation is usually set where the maximum number of counts is recorded, and this may not correspond to the centre of the gate. A consistent criterion must be used for determining the delay used for optimum synchronisation.

Counts in the non-illuminated gates will be solely due to dark counts and after-pulses. A timer/counter, operating in multi-stop mode with dead time less than the time between consecutive detector gates, is triggered by a laser trigger pulse. Collecting data over many scans is used to obtain temporal histograms of laser triggers and detections.

The number of counts in each detector gate is recorded. Counts in a lit gate are denoted by  $C_i$ , and counts in a non-illuminated gate are denoted by  $C_{ni}$ . The number of laser triggers (i.e. scans) is denoted by  $N_{trig}$ .

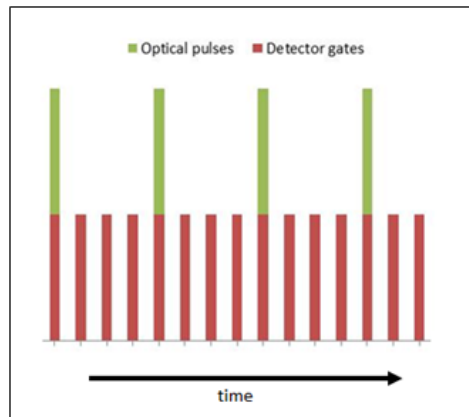


Figure 3.3. Green columns indicate optical pulses, and red columns indicate detector gates. Counts in illuminated gates are due to true detections, after-pulses and detections, whereas counts in non-illuminated gates are due to after-pulses and dark counts.  $R = 4$  in this illustration.

### 3.5.c Calculation

The incident mean photon number is given by:

$$\mu = \frac{P_A 10^{-(A_{hi}-A_{lo})/10}}{f_{source}} \quad (3.2)$$

where

$A_{lo}$  = attenuator attenuation (in dB) when  $P_A$  is measured

$A_{hi}$  = attenuator attenuation for single-photon emission

$P_A$  = measured power for  $A_{lo}$  setting

The after-pulse probability can be calculated from:

$$p_{after} = \frac{C_{ni} - C_{dark}}{C_i - C_{ni}} R \quad (3.3)$$

where

$C_i$  = average number of counts per illuminated gate (true detections + after-pulses + darks),

summed over  $N_{trig}$  scans;

$C_{ni}$  = average number of counts per non-illuminated gate (after-pulses + darks), summed over  $N_{trig}$  scans;

$C_{dark}$  = average number of dark counts per gate, summed over  $N_{trig}$  scans, and calculated from the dark count probability  
 $= N_{trig} \times p_{dark}$ .

In the example of figure 3.3, where each scan covers three complete optical pulse intervals, the values of  $C_i$  can be averaged over 3 lit gates, and the values of  $C_{ni}$  can be averaged over 9 non-illuminated gates.

### 3.6 Detection efficiency

The after-pulse probability and detector efficiency are measured using the same set-up. The basic principle is that the laser pulse frequency  $f_{source}$  is stepped down by an integer factor  $R$  compared to the detector gate rate using a frequency divider. Therefore, only every  $R$ th detector gate will be illuminated. Counts in the unilluminated gates will be solely due to dark counts and after-pulses, while counts in the illuminated gates will be due to true detections, after-pulses, and detections.

A calibrated power is required (Section 3.5) to measure the mean photon number of the incident optical pulses.

#### 3.6.a Measurement

The dark count probability (Section 3.4) and after-pulse probability (Section 3.5) will be required.

The same set-up as described in Section 3.5 for measurement of after-pulse probability is used.

#### 3.4.b Calculation

For pulses from an attenuated laser operating above threshold with a mean number of photons per pulse,  $\mu$ , the probability of there being  $n$  photons in a pulse is assumed to follow the Poissonian distribution, and the probability of a true detection, i.e. one due to the detection of a photon, and not a dark count or after-pulse, is given by (See Appendix 1):

$$p_{true} = 1 - \exp(-\mu\eta) \quad (3.4)$$

where  $\eta$  is the desired detection efficiency. Therefore

$$\eta = -\frac{1}{\mu} \ln(1 - p_{true}) \quad (3.5)$$

The probability of a count in an illuminated gate,  $p_i$ , is given by:

$$p_i = \frac{C_i}{N_{trig}} \quad (3.6)$$

The probability of a true detection is given by:

$$p_{true} = \frac{p_i - p_{dark}}{1 + p_{after}} \quad (3.7)$$

Hence

$$\eta = -\frac{1}{\mu} \ln(1 - p_{true}) = -\frac{1}{\mu} \ln\left(1 - \frac{p_i - p_{dark}}{1 + p_{after}}\right) \quad (3.8)$$

The value of  $\eta$  may need to be adjusted if the detector is subsequently used to measure pulses whose temporal extent is different to that used to calibrate the photon counter; see [24].

### 3.7 Linearity factor (detection efficiency)

The CIE definition of a linear detector is a ‘detector is that for which the output is proportional to the input over a specified range of inputs, so that the responsivity of the detector is constant over that range’ [28]:

The first clause is not directly applicable to non-photon-number-resolving single-photon detectors responding to a photon number distribution, as seen from Eq. (3.4). The second clause which states that the responsivity, i.e. detection efficiency, should be constant, remains valid.

#### 3.7.a Measurement

The mean photon number,  $\mu$ , of the incident optical pulses is varied, and the detection efficiency,  $\eta$ , is measured at each value of  $\mu$ , as described in Sections 3.5 and 3.6.

#### 3.7.b Calculation

Let  $\eta_A$  and  $\eta_B$  be the detector efficiencies for the respective input quantities  $\mu_A, \mu_B$  where  $\mu_A < \mu_B$ . The linearity factor  $F_L(B,A)$  can be defined as the ratio of the detection efficiency at high input flux to that at low input flux, i.e.

$$F_L(B, A) = \frac{\mu_B}{\mu_A} \quad (3.9)$$

If  $F_L$  is unity, the detector is linear across the range of outputs  $N_A$  to  $N_B$ . A value greater than unity indicates super-linearity, and a value less than unity indicates sub-linearity. It is important that the limits  $N_A$  to  $N_B$  over which the measurement has been made are stated.

Where  $\eta_A, \eta_B$  and  $\eta_C$  are measured for  $\mu_A < \mu_B < \mu_C$ , it follows that  $F_L(C,A) = F_L(C, B) \cdot F_L(B,A)$  etc., which can be useful in evaluating the linearity over an extended range of  $\mu$ .

### 3.8 Spectral responsivity

The spectral responsivity, i.e. the detection efficiency measured as a function of wavelength over some spectral range, can be measured using the methods described in Sections 3.5, 3.6 and 2.7. The wavelength of the incident pulses is set to some value, and the DE measured. The wavelength of the incident pulses is then changed, and the DE re-measured, etc.

### 3.9 Dead time, recovery time, partial recovery time, reset time

The dead time, recovery times and reset time can be measured using the two-pulse method. [18,29,30]. A train of double pulses of equal intensity, separated by a tunable time  $\Delta t$ , and attenuated to the single-photon level, are sent to the detector. In the case of gated detectors, the photons will be synchronized to the detector gates, and their time separation incremented in steps equal to a gating period. The probabilities of detecting the first photon,  $p_1$ , the second photon  $p_2$ , and both photons,  $p_{12}$  will be recorded as a function of  $\Delta t$ . The time between pairs of pulses should exceed the expected recovery time, and, in the case of SPAD detectors, ensure a negligible after-pulse probability.

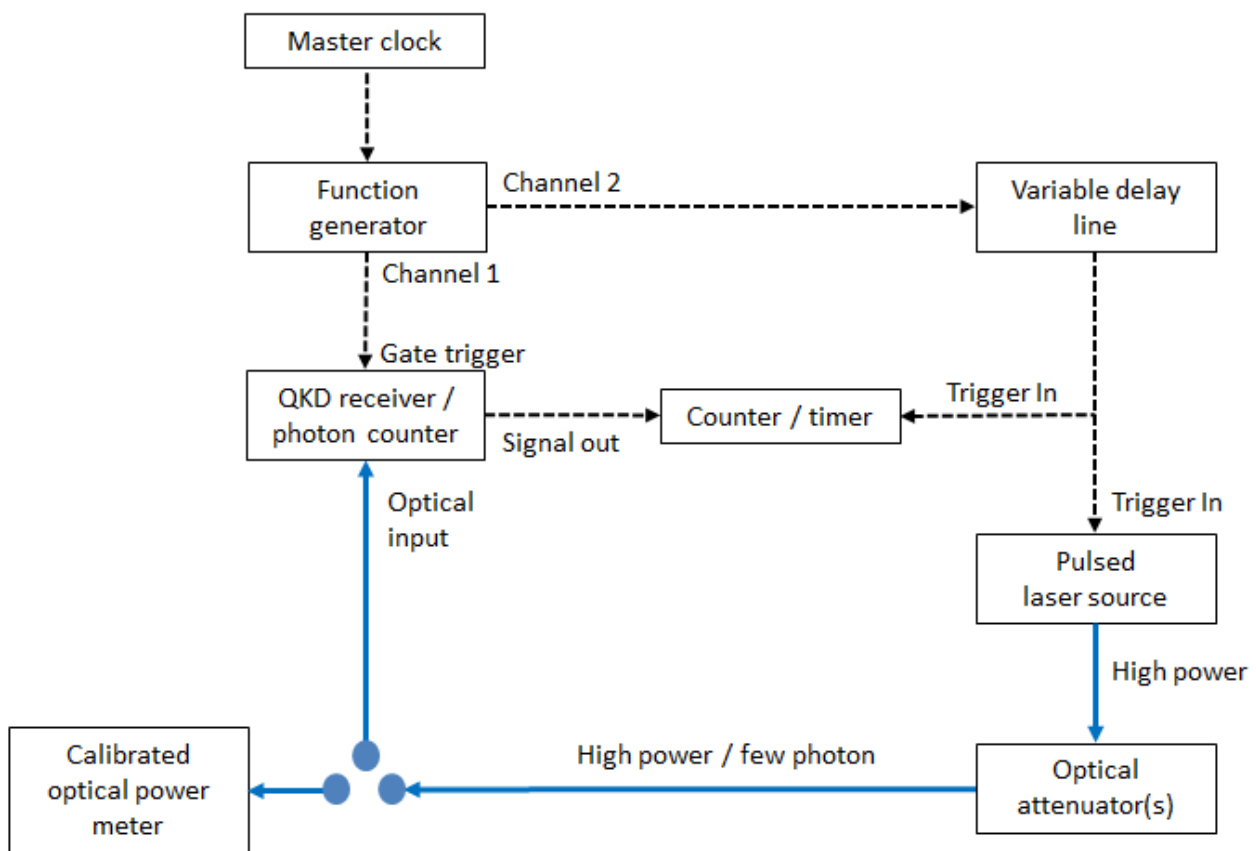


Figure 3.4. Set-up for measurement of dead time and recovery time of QKD photon counter(s). Electronic connections are shown in dashed lines, fibre-optic connections in solid lines. The output of the calibrated optical attenuator can be connected to either the calibrated power meter or the QKD receiver/photon counter. The master clock may be part of the function generator.

#### 3.9.a Required equipment (all fibre-coupled)

- (i) Function generator

A two-channel function generator is required to provide two synchronised signals to trigger the detector gates and the laser.

(ii) Pulsed laser

The laser should operate at the wavelength for which the dead time is required. The duration of the output pulses must be narrower than the duration of the detector gate (see sections 2.10 and 3.3), the narrower the better.

In principle, a CW laser, combined with a means for carving out pulses from this CW output, such as an intensity modulator, can also be used. The duration of these pulses must be narrower than the duration of the detector gate, the narrower the better.

The pulsed laser, or the intensity modulator, must be capable of being driven by an external trigger signal.

(iii) Variable delay line

The variable delay line is used to vary the time delay between the signal used to trigger the detector and the signal used to trigger the laser, in order to synchronise the arrival of the laser pulse within a detector gate. Any jitter introduced by the delay line should not lead to any photons arriving at the detector outside the duration of its gate.

(iv) Calibrated optical attenuator

A calibrated optical attenuator is required to attenuate optical pulses, from the level at which they can be measured with a power meter, to the few-photon level. If a calibrated optical attenuator is not available, it can be calibrated using a calibrated power meter – e.g. see [24].

(v) Counter/timer

The timer/counter must be capable of operating in multi-stop mode with dead time less than the time between consecutive detector gates. The device should be able to generate time histograms of recorded events, or provide raw data from which such histograms can be generated.

### 3.9.b Measurement

The incident optical pulse train is created, and the mean photon number,  $\mu$ , of each pulse is set to a level such that there should be a detection of each incident pulse, i.e.  $\mu\eta > 5$  (see Appendix 1). This may be done with a pulse emitted at the same frequency as the detector gate. See Section 3.5 for guidance on how to achieve this.

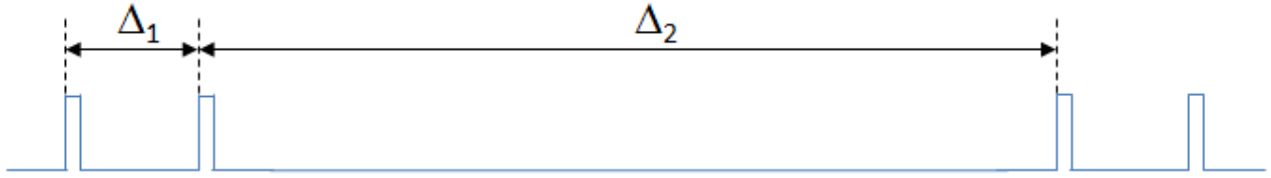


Figure 3.5. Double pulse train:  $\Delta_1$  = spacing between pulses within pair;  $\Delta_2$  = spacing between second pulse of a pair and first pulse of next pair.

An optical pulse train with :  $\Delta_1 = 1$  (in units of gate intervals), and  $\Delta_2 \gg t_{\text{recovery}}$  (expected) is then created and synchronised with the detector gates.

A timer/counter, operating in multi-stop mode with dead time less than the time between consecutive detector gates, is triggered by one of the laser pulse triggers (e.g. the first pulse trigger). The time-span over which stop events is collected must be long enough to collect detection events corresponding to at least one pulse pair. Repeated triggering is used to obtain a temporal histogram of detections. The number of counts corresponding to detections of the first pulse of the pulse pair is denoted by  $C_1$ , the number of counts corresponding to detections of the second pulse of the pulse pair gate is denoted by  $C_2$ , and the number of counts corresponding to detections of both pulses of the pulse pair gate is denoted by  $C_{12}$ . The number of laser triggers (i.e. scans) is denoted by  $N_{\text{trig}}$ .  $\Delta_1$  is then successively incremented by one gate interval, and the measurement repeated.

### 3.9.c Calculation

For a given value of  $\Delta_1$ ,

$$p_1 = C_1 / N_{\text{trig}} - p_{\text{dark}} \quad (3.10)$$

$$p_2 = C_2 / N_{\text{trig}} - p_{\text{dark}} (1 + p_{\text{after}}) - p_1 p_{\text{after}} \quad (3.11)$$

$$p_{12} = C_{12} / N_{\text{trig}} - p_1 p_{\text{dark}} - p_2 p_{\text{dark}} - p_1^2 p_{\text{after}} - 2 p_1 p_{\text{dark}} p_{\text{after}} - p_{\text{dark}}^2 - p_{\text{dark}}^2 p_{\text{after}} \quad (3.12)$$

where  $p_{\text{dark}}$  is the dark count probability, and the after-pulse probability  $p_{\text{after}}$  is the value for the particular value of  $\Delta_1$  employed.

The last three terms in (3.12) can be ignored if  $p_1, p_2 \gg p_{\text{dark}}, p_{\text{after}}$ , as is usually the case. See Appendix 3 for the derivations of 3.12.

### 3.9.d Dead time

The dead time  $t_{\text{dead}}$  is the value of  $\Delta_1$  at which  $C_{12}$  becomes non-zero.

### 3.9.e Recovery time

The recovery time  $t_{\text{recovery}}$  is the value of  $\Delta_1$  at which  $p_{12} = p_1^2$ , i.e.  $p_1 = p_2$ .

### 3.9.f Partial recovery time

The partial recovery time can be chosen to be the time at which  $p_2$  becomes a certain sub-unity multiple of  $p_1$ , e.g. 0.9 or 0.99,

i.e. the partial recovery time  $t_{\text{partialrecovery}}$  is the value of  $\Delta_1$  at which  $p_{12} = \text{PR } p_1^2$ , i.e.  $p_2 = \text{PR } p_1$ , where PR is selected to some value less than 1, such as 0.9 or 0.99.

### 3.9.g Reset time

The reset time  $t_{\text{reset}}$  is given by  $t_{\text{reset}} = t_{\text{recovery}} - t_{\text{dead}}$

## 3.10 Maximum count rate

### 3.12.a Equipment required

- a pulse generator
- a pulsed laser plus an optical attenuator
- counter

### 3.12.b Measurement

Measurement of the achievable maximum count rate of a gated detector with a specific fixed value of the dead time is performed by carrying out the following steps:

Illuminate the detector with laser pulses at the same frequency as the detector gate frequency. Use the attenuator to increase the number of photons per pulse to achieve unit probability of having a click per pulse/gate.

Increase the gate/pulse frequency while expecting to observe a linear increase in the count rate. Once a distortion in the expected linear behaviour is observed (namely of 10%) this will correspond to the maximum count rate of the detector for that specified value of the dead time.

## 3.11 Timing jitter

Measurement can be carried out with a pulsed laser after attenuation to the single-photon level.

The measurement set-up is shown in figure 3.6

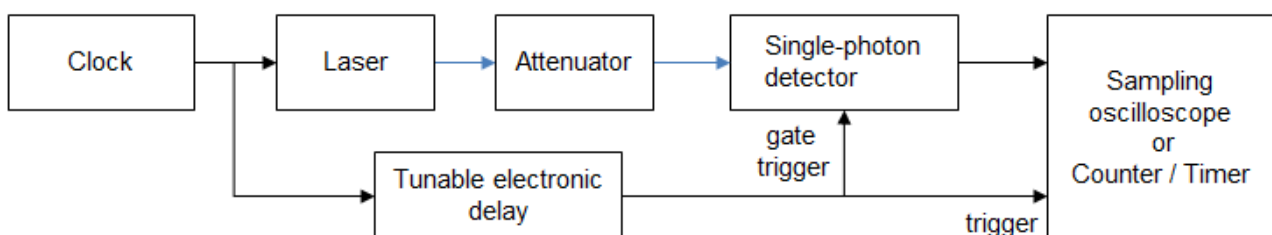


Figure 3.6 Experimental set-up

### 3.13.a Required equipment

(i) Master clock.

This could be an external device, or an internal clock within the DUT which is used to drive the laser, and which is also accessible to trigger the detector and counter/timer.

(ii) Pulsed laser.

The laser should operate at the wavelength for which the detection efficiency is required to be measured. The duration of the output pulses must be narrower than the duration of the detector gate (see sections 2.10 and 3.3), the narrower the better.

In principle, a CW laser, combined with a means for carving out pulses from this CW output, such as an intensity modulator, can also be used. The duration of these pulses must be narrower than the duration of the detector gate, the narrower the better. Hence, an equal duty cycle modulation signal will not be appropriate.

The pulsed laser, or the intensity modulator, must be capable of being driven by an external clock signal.

(iii) Calibrated optical attenuator

A calibrated optical attenuator is required to attenuate optical pulses to the single photon level. See Sections 3.5 and 3.6 for full details, and ancillary equipment that may be required.

(iv) Variable delay line

The variable delay line is used to vary the time delay between the signal used to trigger the detector and the signal used to trigger the laser, in order to synchronise the arrival of the laser pulse within a detector gate. Jitter introduced by the delay line should not lead to any photons arriving at the detector outside the duration of its gate.

(vi) High-bandwidth photodiode

(vii) Counter/timer

The timer/counter should be able to generate histograms of recorded events as a function of time relative to the trigger pulses, or provide raw data from which such histograms can be generated. The temporal resolution of the timer/counter should be such that the observed full-width at half-maximum (FWHM) of the histogram spans a minimum of 10 time bins.

- (vii) High-bandwidth sampling oscilloscope

### **3.13.b Measurement**

The set-up shown in figure 3.6 is used, but with the high-bandwidth photodiode used in place of the single-photon detector (DUT). The temporal profile of the source emission with respect to the trigger (after transmission through the delay line) is measured before attenuation to the single-photon level, as described in Section 2.10.2.

The laser pulses are then attenuated to the single-photon level (Section 3.3), and the photodiode replaced with the single-photon detector. The tunable electronic delay is used to synchronise the arrival of pulses within the detector bias gates.

Measurements can be carried out for the pulses incident at different times within the detector gate (Section 3.3) to see if the detector jitter varies as function of pulse position within the gate.

#### **3.13.b.1 Measurement with oscilloscope**

The oscilloscope is set to a mode such that a histogram of sampled points from the trace produced by the photodiode, as a function of time relative to the trigger, is accumulated.

The mean signal level for each time-delay is then calculated to obtain the resulting response curve.

This curve is the temporal response profile due to the source emission temporal profile, the detector signal jitter, and any jitter due to the oscilloscope (assumed to be negligible).

#### **3.13.c.1 Calculation**

The source emission temporal profile is deconvolved from the measured signal, which yields the jitter.

The span and standard deviation of the falling edge histogram gives the peak-to-peak and standard deviation jitter.

#### **3.13.b.2 Measurement with counter/timer**

A histogram of detection times will be observed by correlating many successive detection events with the clock trigger signal. The histogram is the temporal response profile due to the source emission temporal profile, the detector signal jitter, and jitter due to the timer/counter.

### **3.13.c.2 Calculation**

The source emission temporal profile is deconvolved from the measured signal. The jitter due to the counter/timer is expected to be negligible.

The span and standard deviation of the resulting curve gives the peak-to-peak and standard deviation jitter.

# Appendix 1

## Derivation of $p_{det} = 1 - \exp(-\mu\eta)$ [31,32]

The number of photons in an attenuated laser pulse is taken to have the Poissonian distribution. This means that the probability  $p(n)$  of there being exactly  $n$  photons in a pulse, where the mean number of photons in a pulse for the parent distribution is  $\mu$ , is given by

$$p(n) = \frac{\mu^n e^{-\mu}}{n!} \quad (A1.1)$$

A non-photon-number-resolving single-photon detector produces an output signal once a photon is detected. If a pulse containing  $n$  photons is incident on such a detector with detection efficiency  $\eta$ , the probability of producing a signal from the  $m^{\text{th}}$  photon ( $m \leq n$ ) is the probability of not detecting the previous  $(m-1)$  photons multiplied by the probability of detecting the  $m^{\text{th}}$  photon, i.e.

the probability of producing an output signal from the first photon is	$\eta$
the probability of producing an output signal from the second photon is	$(1-\eta)\eta$
the probability of producing an output signal from the third photon is	$(1-\eta)^2\eta$
...	
the probability of producing an output signal from the $n^{\text{th}}$ photon is	$(1-\eta)^{n-1}\eta$

Hence, the probability of producing an output signal  $s(n)$  from a pulse containing  $n$  photons is given by:

$$\begin{aligned} s(n) &= \eta + (1-\eta)\eta + (1-\eta)^2\eta + \dots + (1-\eta)^{n-1}\eta \\ &= \eta[1 + (1-\eta) + (1-\eta)^2 + \dots + (1-\eta)^{n-1}] \\ &= 1 - (1-\eta)^n \end{aligned} \quad (A1.2)$$

using the relationship  $S_n = a \frac{1-r^n}{1-r}$  for summing an  $n$ -term geometric progression, where  $a = \eta$  and  $r = (1-\eta)$

We can consider a pulse of mean photon number  $n$  incident on a detector of detection efficiency  $\mu$  as being equivalent to a pulse of mean photon number  $n\mu$  being incident on a detector of detection efficiency 1. (Formally, we consider a Poissonian distribution of mean photon number  $n$  incident upon a lossless beamsplitter of transmittance  $\mu$ . The transmittance/reflectance of the beamsplitter follows a Bernoulli process, which leads to a transmitted distribution which remains Poissonian, but which now has a mean photon number  $\eta\mu$ ). Therefore, the probability of an output signal  $p_{det}$  from a pulse of mean photon number  $n$  reduces to one minus the probability of there being no photons in an incident Poissonian distribution of mean photon number  $\eta\mu$ .

$$p_{det} = 1 - \left. \frac{(\eta\mu)^n e^{-\eta\mu}}{n!} \right|_{n=0} = 1 - e^{-\eta\mu} \quad (A1.3)$$

The same result can be found as shown in equation A1.4:

$$p_{\text{det}} = \sum_{n=0}^{\infty} [s(n) p(n)] = 1 - e^{-\eta\mu} \quad (\text{A1.4})$$

## Appendix 2

### Derivation of Eq. 2.6

The detection probability  $p^{det}$  for a pulse for a specific mean photon level setting is recorded, where

$$p^{det} = \frac{N_{det}}{N_{gates}}, \quad (A2.1)$$

with  $N_{det}$ : number of detections in  $N_{gates}$ ,  $N_{gates}$ : number of illuminated gates.

The number of detections  $N_{det}$  contains also dark counts and after-pulses:

$$N_{dark} = N_{gates} p^{dc} \quad (A2.2)$$

$$N_{after} = (N_{true} + N_{dark}) p^{after} \quad (A2.3)$$

where

$p^{dc}$ : dark count probability;

$N_{dark}$ : number of dark counts;

$p^{after}$ : after-pulse probability;

$N_{after}$ : number of afterpulses;

$N_{true}$ : number of true photon events.

Therefore:

$$N_{det} = (N_{true} + N_{dark})(1 + p^{after}) \quad (A2.4)$$

The number of true detection events is given by:

$$N_{true} = \frac{N_{det}}{1 + p^{after}} - N_{dark} \quad (A2.5)$$

The probability of a true detection is therefore given by:

$$\frac{N_{true}}{N_{gates}} = \frac{p^{det}}{1 + p^{after}} - p^{dc} \quad (A2.6)$$

For a Poissonian distribution with a mean number  $\mu$  of photons in a pulse, the following relation holds:

$$\frac{N_{true}}{N_{gates}} = 1 - \exp(-\mu\eta_D) \quad (A2.7)$$

where  $\eta_D$  is the detection efficiency of the photon counter.

Therefore, the mean photon number is given by:

$$\mu = \frac{1}{\eta_D} \ln \left( 1 - \frac{N_{true}}{N_{gates}} \right) = \frac{1}{\eta_D} \ln \left\{ 1 - \frac{p^{det}}{1 + p^{after}} + p^{dc} \right\} \quad (A2.8)$$

Additional corrections may be needed to take account of detector recovery efficiency.

## Appendix 3

Derivation of Eq. (3.10 – 3.12)

$$C_1 = p_1 N_{trig} + p_{dark} N_{trig}$$

$$p_1 = \frac{C_1}{N_{trig}} - p_{dark}$$

$$C_2 = p_2 N_{trig} + p_{dark} N_{trig} + p_{after} C_1 = p_2 N_{trig} + p_{dark} N_{trig} + p_1 p_{after} N_{trig} + p_{dark} p_{after} N_{trig}$$

$$p_2 = \frac{C_2}{N_{trig}} - p_{dark} - p_1 p_{after} - p_{dark} p_{after}$$

$$\frac{C_{12}}{N_{trig}} = \frac{C_1}{N_{trig}} \frac{C_2}{N_{trig}}$$

$$= (p_1 + p_{dark})(p_2 + p_{dark} + p_1 p_{after} + p_{dark} p_{after})$$

$$= p_1 p_2 + p_1 p_{dark} + p_1^2 p_{after} + p_1 p_{dark} p_{after} + p_2 p_{dark} + p_{dark}^2 + p_1 p_{dark} p_{after} + p_{dark}^2 p_{after}$$

$$p_{12} = \frac{C_{12}}{N_{trig}} - p_1 p_{dark} - p_2 p_{dark} - p_1^2 p_{after} - 2p_1 p_{dark} p_{after} - p_{dark}^2 - p_{dark}^2 p_{after}$$

## Appendix 4

### Photon indistinguishability

Let  $P^A(x)$  and  $P^B(x)$  describe the distributions of photons A and B respectively, with respect to some parameter  $x$ , such that

$$\int_x P^A(x)dx = \int_x P^B(x)dx = 1 \quad (\text{A4.1})$$

The indistinguishability for the photons, labelled A and B, can be defined as [33]:

$$x^{ind} = 1 - \frac{1}{2} \int |P^A(x) - P^B(x)| dx \quad (\text{A4.2})$$

$x^{ind} = 1$  for perfect indistinguishability, and  $x^{ind} = 0$  for perfect distinguishability (no overlap in parameter  $x$ ).

## References

1. P D Townsend, J G Rarity, and P R Tapster 1993 Single photon interference in 10 km long optical fibre interferometer *Electronics Letters* **29**(7), 634-635.
2. G Brassard, N Lutkenhaus, T Mor, and B C Sanders 2000 Limitations on practical quantum cryptography *Phys. Rev. Lett.* **85**(6), 1330-1333.
3. V Scarani, A Acin, G Ribordy, and N Gisin 2004 Quantum cryptography protocols robust against photon number splitting attacks for weak laser pulse implementations *Phys. Rev. Lett.* **92**(5), 057901.
4. H-K Lo, X Ma, and K Chen 2005 Decoy state quantum key distribution *Phys. Rev. Lett.* **94**(23), 230504.
5. S Cova, A Longoni, and A Andreoni 1981 Towards picoseconds resolution with single-photon avalanche diodes *Rev. Sci. Instrum.* **52**(3), 408-412.
6. R G W Brown, K D Ridley, and J G Rarity 1986 Characterization of silicon avalanche photodiodes for photon correlation measurements. 1: Passive quenching *Appl. Opt.* **25**(22), 4122-4126.
7. R G W Brown, R Jones, J G Rarity, and K D Ridley 1987 Characterization of silicon avalanche photodiodes for photon correlation measurements. 2. Active quenching *Appl. Opt.* **26**(12), 2383-2389.
8. S Cova, M Ghioni, A Lotito, I Rech, and F Zappa 2004 Evolution and prospects for single-photon avalanche diodes and quenching circuits *J. Mod. Optics* **51**(9-10), 1267-1288.
9. A Lacaita, F Zappa, S Cova, and P Lovati 1996 Single-photon detection beyond 1  $\mu\text{m}$ : performance of commercially available InGaAs/InP detectors *Appl. Opt.* **35**(16), 2986-2996.
10. G Ribordy, J-D Gautier, H Zbinden, and N Gisin 1998 Performance of InGaAs/InP avalanche photodiodes as gated-mode photon counters *Appl. Opt.* **37**(12), 2272-2277.
11. J G Rarity, T E Wall, K D Ridley, P C M Owens, and P R Tapster 2000 Single-photon counting for the 1300-1600-nm range by use of Peltier-cooled and passively quenched InGaAs avalanche photodiodes *Appl. Opt.* **39**(36), 6746-6753.
12. P A Hiskett, G S Buller, A Y Loudon, J M Smith, I Gontijo, A C Walker, P D Townsend, and M J Robertson 2000 Performance and design of InGaAs/InP photodiodes for single-photon counting at 1.55  $\mu\text{m}$  *Appl. Opt.* **39**(36), 6818-6829.
13. M A Itzler, X Jiang, M Entwistle, K Slomkowski, A Tosi, F Acerbi, F Zappa, and S Cova 2011 Advances in InGaAsP-based avalanche diode single photon detectors *J. Mod. Optics* **58**(3-4), 174-200.
14. R T Thew, D Stucki, J-D Gautier, H Zbinden, and A Rochas 2007 Free-running InGaAs/InP avalanche photodiode with active quenching for single photon counting at telecom wavelengths *Appl. Phys. Lett.* **91**(20), 201114.
15. R E Warburton, M Itzler, and G S Buller 2009 Free-running room temperature operation of an InGaAs/InP single-photon avalanche diode *Appl. Phys. Lett.* **94**(7), 071116.
16. M A Itzler, X Jiang, and M Entwistle 2012 Power law temporal dependence of InGaAs/InP SPAD afterpulsing *J. Mod. Optics* **59**(17), 1472-1480.
17. A Migdall, S V Polyakov, J Fan, and J C Bienfang (Eds), *Single-Photon Generation and Detection: Physics and Applications*, Academic Press, Oxford, (2013).
18. A R Dixon, J F Dynes, Z L Yuan, A W Sharpe, A J Bennett, and A J Shields 2009 Ultrashort dead time of photon-counting InGaAs avalanche photodiodes *Appl. Phys. Lett.* **94**(23), 231113.
19. R H Hadfield 2010 single-photon detectors for optical quantum information applications *Nature Photonics* **3**, 696-705.
20. Z L Yuan, B E Kardynal, A W Sharpe, and A J Shields 2007 High speed single photon detection in the near infrared *Appl. Phys. Lett.* **91**(4), 041114-041113.

21. ID220 FREE RUNNING SINGLE PHOTON DETECTOR  
<http://www.idquantique.com/photon-counting/photon-counting-modules.html?id=145>,  
accessed on 10 Sep 2014
22. ID230 FREE RUNNING SINGLE PHOTON DETECTOR  
<http://www.idquantique.com/photon-counting/photon-counting-modules.html?id=321>,  
accessed on 10 Sep 2014
23. J F Dynes, I Choi, A W Sharpe, A R Dixon, Z L Yuan, M Fujiwara, M Sasaki, and A J Shields 2012 Stability of high bit rate quantum key distribution on installed fiber *Opt. Exp.* **20**(15), 16339-16347.
24. C J Chunnillall, G Lepert, J J Allerton, C J Hart, and A G Sinclair 2014 Traceable metrology for characterizing quantum optical communication devices *Metrologia* **51**(6), S258.
25. E A Dauler, M E Grein, A J Kerman, F Marsili, S Miki, S W Nam, M D Shaw, H Terai, V B Verma, and T Yamashita 2014 Review of superconducting nanowire single-photon detector system design options and demonstrated performance *Opt. Eng.* **53**(8), 081907-081907.
26. C M Natarajan, M G Tanner, and R H Hadfield 2012 Superconducting nanowire single-photon detectors - physics and applications *Supercond. Sci. Technol.* **25**(6), 063001.
27. P Grangier, G Roger, and A Aspect 1986 Experimental Evidence for a Photon Anticorrelation Effect on a Beam Splitter: A New Light on Single-Photon Interferences. *Europhys. Lett.* **1**(4), 173-179.
28. CIE, Standard CIE S 017/E:2011 ILV: International Lighting Vocabulary, Babenbergerstraße 9/9A, A-1010 Vienna, Austria, 2011. <http://eilm.cie.co.at/>
29. J Zhang, W Slysz, A Verevkin, O Okunev, G Chulkova, A Korneev, A Lipatov, G N Gol'tsman, and R Sobolewski 2003 Response time characterization of NbN superconducting single-photon detectors *IEEE Trans. Appl. Supercond.* **13**(2), 180-183.
30. A J Kerman, E A Dauler, W E Keicher, J K W Yang, K K Berggren, G Gol'tsman, and B Voronov 2006 Kinetic-inductance-limited reset time of superconducting nanowire photon counters *Appl. Phys. Lett.* **88**(11), 111116.
31. H B Coldenstrodt-Ronge and C Silberhorn 2007 Avalanche Photo-Detection for High Data Rate Applications *J. Phys. B: At. Mol. Phys.* **40**(19), 3909.
32. W Schmunk, M Rodenburger, S Peters, H Hofer, and S Kück 2011 Radiometric calibration of single photon detectors by a single photon source based on NV-centers in diamond *J. Mod. Optics* **58**(14), 1252-1259.
33. Z L Yuan, J Y Cheung, T Debuisschert, I P Degiovanni, J-M Merolla, A Poppe, A J Shields, and A G Sinclair, Quantum Key Distribution (QKD); Components and Internal Interfaces Group Specification Report No. ETSI GS QKD 003 v1.1.1 (2010-12), 650 Route des Lucioles, F-06921 Sophia Antipolis Cedex - FRANCE, 2010.  
<http://www.etsi.org/technologies-clusters/technologies/quantum-key-distribution>